

Distances of Galactic Radio Pulsars; First Quadrant: $-2^\circ < \ell < 90^\circ$ and $-2^\circ < b < 2^\circ$

Pınar Kütükçü,^{1*} Aşkın Ankaş,² Efe Yazgan³ and Kutsal Bozkurt¹

¹Physics Department, Yıldız Technical University, Davutpaşa Cad., 34220, Esenler/Istanbul, Turkey

²Physics Department, Boğaziçi University, North Campus, KB Building Floor 3-4, 34342 Bebek/Istanbul, Turkey

³Physics Department, National Taiwan University, Taipei, Taiwan

Accepted XXX. Received YYY; in original form ZZZ

ABSTRACT

Distance versus dispersion measure relations are constructed for Galactic radio pulsars in small solid angle intervals. The calculations are based on some basic criteria as well as using the independent distance measurements of well examined pulsars for the first Galactic quadrant including Galactic central directions. Values of average free electron density for these regions are derived from the fits to distance versus dispersion measure relations and checked for consistency and smoothness. The effects of plasma in the Galactic arms and within the central parts of the Galactic bulge region are also compared and discussed. Our adopted distances for the radio pulsars are compared with the ones given in some other models. Some basic results on distributions of the radio pulsars and the plasma are presented.

Key words: stars: neutron – ISM: structure – Galaxy: structure – stars: distances – HII regions – methods: statistical

1 INTRODUCTION

Since the first observation of a pulsar (PSR) in 1967, more than 2800 pulsars were observed up to date according to the ATNFPC (Australia Telescope National Facility Pulsar Catalog) (Manchester et al. 2005). Most of these pulsars are observable at radio frequencies due to their synchrotron emission. It is essential to know the distances of pulsars from the Sun mainly in order to calculate their radiative power and to determine their positions and distributions in the Galaxy.

Most of the known pulsars are isolated objects and none of the directly observable intrinsic properties of pulsars allows for a distance determination of a pulsar unlike some other sources, e.g. cepheids. For a few of the pulsars that are close enough, the parallax method could be utilized. Because of the high speeds of neutron stars gained during asymmetric core-collapse supernova explosions and the short observable lifetimes (10^4 - 10^5 yr) of supernova remnants (SNRs) (Guseinov et al. 2007), only young neutron stars can reliably be associated to SNRs. As the number of Galactic SNRs including neutron stars, pulsar wind nebulae and/or bow shock structures is not more than half of the known SNRs (Green 2019) and the fact that SNR distances are not small in most of the cases (Guseinov et al. 2007, and references therein, Ranasinghe & Leahy 2018, Green 2019, and references therein, Lee et al. 2019), there are only a few neutron star – SNR pairs with reliable distances. The distances of pulsars located in globular clusters can be determined with a better precision, however the observed number of such pulsars is small.

In this work, we present an improved version of a basic and reliable method to determine distances of all radio pulsars with known dispersion measure (DM) values based on constructing distance – DM relations (Yazgan et al. 2007; Ankaş et al. 2016). It is possible

to derive average free electron densities in the line of sight (LOS) of the radio pulsars from these relations to constrain the distributions of the plasma as well as the radio pulsars in the Galaxy. Figures and tables for distance-DM relations in the solid angle interval $2^\circ < \ell < 90^\circ$; $-2^\circ < b < 2^\circ$ are given in Appendix A.

Most of the pulsars listed in the ATNFPC have precise timing observations that allow distance determinations based on the 3D free electron distributions. Passing through the interstellar plasma, radio waves from pulsars get dispersed depending on the electron density along the line of sight and the frequency of the radio pulse (ν). Thanks to the pulsed emission, the difference in the arrival times between two frequencies, both much greater than the plasma frequency, is measurable. This delay Δt can be written as (Lipunov 1992)

$$\Delta t = t_2 - t_1 = \left(\frac{1}{\nu_2^2} - \frac{1}{\nu_1^2} \right) \frac{e^2}{2m_e c} \int_0^D n_e ds \quad (1)$$

The last term in equation (1) is defined as DM in pc/cm^3 :

$$DM \equiv \int_0^D n_e ds \quad (2)$$

Here c is the speed of light in vacuum, m_e is the mass of electron, e is the electron charge, n_e is the free electron density in the LOS in cm^{-3} , and D is the distance of the radio pulsar from the Sun. Distance of the source can be found using this equation if the electron density in the LOS is known.

This method is practically applicable only in the case of pulsed low frequency emission making it the standard method applicable to all radio pulsars as a rule. The DM measurements have in general

* E-mail: pinarkutukcu@gmail.com

small inaccuracies and the variations in the DM values due to displacements of filaments in SNRs are rare and mostly insignificant (Petroff et al. 2013). The main and effectively the only difficulty in using this method is related to the mostly unknown distributions of the plasma regions (mainly SNRs and HII-regions) throughout the Galaxy and their densities. The first mathematical model on DM-based distance determination (Taylor & Cordes 1993) used in ATNFPC led to overestimated and underestimated distance values especially in the Galactic center directions. An improved version of such a model was introduced by Cordes & Lazio (2002), yet this model also gives overestimated/underestimated pulsar distances. The plasma distribution in our galaxy, though it is relatively more uniform compared to the distributions of molecular clouds and HI clouds, can not be adequately described by simple mathematical models using general assumptions. However, the models are being improved, e.g. as introduced in Yao et al. (2017) (YMW17 model) which is the latest model used in ATNFPC as the default model. This model also includes systematic biases which are discussed below.

Alternatively, distance – DM relations can be constructed for small solid angles choosing narrow longitude and latitude intervals including pulsars with measured DM to fit and using the independently measured distance values of calibrator pulsars (e.g. Yazgan et al. 2007; Guseinov et al. 2002; Ankay et al. 2016). The average free electron number density values can be determined from these relations for a large number of solid angle intervals covering the whole galaxy. The criteria mainly introduced by Guseinov et al. (2002) and Yazgan et al. (2007) in adopting distances for some radio pulsars with measured DM values with some improvements will be presented below.

The rotation measure (RM) based on the Faraday rotation is also a precisely measured quantity similar to DM but for a smaller number of pulsars. RM depends on the average magnetic field of the interstellar medium in the LOS as well as the average free electron density. So the ratio RM/DM gives information on the average magnetic field of the interstellar medium which can in principle be used to check and compare the distance values of pulsars located in the same region (Manchester and Taylor (1977)). RM is defined through the following equations:

$$RM \equiv \frac{e^3}{2\pi m_e^2 c^4} \int_0^D n_e B \cos\theta ds \quad (3)$$

$$\langle B \cos\theta \rangle = 1.232 \frac{RM}{DM} \quad (4)$$

Here B is the magnetic field strength and θ is the angle between the line of sight and the magnetic field. The unit of B is μG and the unit of RM is rad/m^2 .

Having a precise knowledge of the locations and the sizes of the Galactic arms is essential to determine both the Galactic plasma (in particular the free electron density) distribution and the locations of Galactic young pulsars. Giant molecular clouds, HII regions and masers are used as the basic sources and tracers in most of the Galactic arms structure models (e.g. Georgelin & Georgelin 1976; Reardon et al. 2016a; Hou et al. 2009; Xu et al. 2013; Zhang et al. 2013; Choi et al. 2014; García et al. 2014; Hou & Han 2014; Reid et al. 2014; Sato et al. 2014; Vallée 2014a,b; Wu et al. 2014; Hachisuka et al. 2015; Vallée 2015, and references therein).

Recent observations (Ponti et al. 2015; Schnitzeler et al. 2016), found that the plasma at the core of the Galactic bulge is very dense, probably denser than the plasma in the most dense parts of the Galactic arms, including some "holes" with low density. This is discussed

below based on the observations of radio pulsars close to or in the direction of the Galactic center especially a magnetar which is probably connected to the dense plasma region Sgr A located at the center.

2 BASIC CRITERIA IN ADOPTING DISTANCES OF RADIO PULSARS AND ITS RELATION TO THE GALACTIC PLASMA DISTRIBUTION

We have constructed distance – DM relations for radio pulsars in the first quadrant of the Galaxy for $b = 0 \pm 2$ degrees including also the Galactic central directions in the intervals $\ell = b = 0 \pm 2$ degrees. We have divided the pulsars into 20 groups, each group having 4 degrees by 4 degrees solid angle, up to $\ell = 78$ degrees. The average free electron density for each group has been calculated and compared with each other for adjacent groups to check the smoothness and continuity of the plasma distribution. The number of radio pulsars in the longitude interval $\Delta\ell = 78-90$ degrees with $b = 0 \pm 2$ degrees is only three, therefore, we have only checked the possible distances of these pulsars without making a fit.

Some basic criteria based on observational results are listed below to construct distance versus DM relations (Ankay et al. 2016). We assume that the main contribution to the measured DM values is mainly due to the plasma in the HII regions, SNRs and probably the Galactic central region. A low density plasma distribution between the Galactic arms and at high latitudes are also taken into consideration.

The first and the fourth quadrants of the Galaxy must include most of the radio pulsars, and in general most of the Galactic sources, as the volume of this region is significantly larger than the anti-center region. This is also the case for young pulsars as they are supposed to be located within or close to the star formation regions (SFRs) that form the Galactic arms. On the other hand, as the Galactic arm structure beyond the Galactic center is not well known in the first and the fourth quadrants, it is much more difficult to determine the locations of distant pulsars. Yet, some of the most luminous radio pulsars are definitely located in the interval $-40^\circ < \ell < 40^\circ$. Based on the available observational data (ATNFPC), the number of such luminous pulsars in this interval is not as large as expected suggesting that a larger portion of the Galactic arms are outside of this longitude interval. The distribution of the space velocities of pulsars and the activity of the star formation regions producing core-collapse supernovae are considered to get a conclusive result.

In order to have an estimate on the radio pulsar luminosity, we take Crab pulsar as a reference to put an upper limit for each radio pulsar distance using the measured fluxes at 1400 MHz and 400 MHz. Crab pulsar is taken as a reference to put an upper limit because it is close by and young. Its well-known luminosity helps prevent large overestimation in adopting pulsar distances. About 96% of radio pulsars are less luminous than the Crab pulsar at 400 MHz and about 87% radio pulsars are less luminous than Crab pulsar at 1400 MHz (ATNFPC). For almost all of the radio pulsars, the 1400 MHz distance limit is much smaller than the one at 400 MHz. Therefore, the luminosity of the Crab pulsar can be used as a lower limit to prevent large over-estimations in adopting pulsar distances. Guseinov et al. (2003a) constructed luminosity functions for young radio pulsars ($\tau < 10^7$ yr) at 400 MHz and 1400 MHz and showed that most of the PSRs have low luminosity values. For a detailed review on pulsar luminosities see Bagchi (2013).

In some Galactic longitude intervals, some parts of the arms are offset with respect to the Galactic plane. Some of these deviations are well known by observation, especially at smaller distances from

the Sun, and are considered both for the free electron distribution in the Galaxy and when adopting radio pulsar distances.

The distances of pulsars from the Galactic plane are related to their ages. The spin-down age of a pulsar is given by

$$t = \frac{P}{(n-1)\dot{P}} \left[1 - \left(\frac{P_0}{P} \right)^{(n-1)} \right] \quad (5)$$

where n is the braking index, P is the period, P_0 is the birth period and \dot{P} is the time derivative of the period of the pulsar. Assuming $P_0 \ll P$ and $n \neq 1$

$$t = \frac{1}{(n-1)} \frac{P}{\dot{P}} \quad (6)$$

The characteristic age is defined for $n=3$ (for magnetic dipole braking) as (Manchester & Taylor 1977; Lyne & Graham-Smith 2012)

$$\tau = \frac{P}{2\dot{P}} \quad (7)$$

Note that the characteristic age is not a measure of the true age (Jiang et al. 2013). For example, for the Crab pulsar $\tau=1256.8$ yr (ATNFPC) and the real age is equal to the age of SN 1054 which is ~ 970 yr. Espinoza et al. (2011) give a list of young galactic pulsars with reliable measured braking indices in the range 2.14-2.91. So, the real age can be greater than τ up to a factor of 2 based on these measured values of braking index. Such small differences in age values do not affect our analysis or change our results in this work. For the pulsar J1734-3333 Espinoza et al. (2011) measure a braking index value 0.9, mentioning a recent glitch would most likely disrupt the \dot{P} value. Lyne et al. (1996) give a braking index value 1.4 for the Vela pulsar (J0835-4510), where they mention a large uncertainty in the \dot{P} measurement caused by glitch together with the timing noise. For J1640-4631 ($\tau=3.35 \times 10^3$ yr (ATNFPC)), Archibald et al. (2016) measure a braking index value 3.15 and argue the reason of a high braking index value may occur because of an unseen glitch when the timing noise is ignored. This braking index value for J1640-4631 must be in accordance with energy loss due to pure magnetic dipole radiation within uncertainties. For a similar example for characteristic age and real age values (J1801-2451), see section 3.2. According to Guseinov et al. (2004) magnetic fields of pulsars decay exponentially and the characteristic time scale for this process is about 3×10^6 yr. As shown by Guseinov et al. (2004), the correlation between τ and the kinematic age (depending on the pulsar distance from the plane) no longer exists for $\tau > 10^7$ years. This is also considered in adopting distances of older pulsars, in particular for the ones in the regions of the Galactic arms that are deviated from the Galactic plane.

According to Faucher-Giguère & Kaspi (2006) average space velocity of pulsars is 380_{-60}^{+40} km/s. Verbunt et al. (2017) suggest that the average space velocity of 42% of pulsars is 120 km/s and 58% of pulsars is 580 km/s. There are 422 PSRs whose transverse speed (V_{trans}) is given according to the adopted distances by the ATNFPC and the average value of the transverse speeds of these pulsars is 265.7 km/s. There are some very large V_{trans} values given in ATNFPC (e.g. PSR J1327-0755 $V_{trans}=11705$ km/s, $b=53.848^\circ$, $d>25$ kpc; PSR J0134-2937 $V_{trans}=2279.86$ km/s, $b=-80.250^\circ$, $d>25$ kpc; PSR J0151-06354 $V_{trans}=1419.49$ km/s, $b=-65.004^\circ$, $d>25$ kpc; PSR J2116+1414 $V_{trans}=1612.10$ km/s, $b=-23.409^\circ$, $d>25$ kpc). This is mainly because of some of the PSRs with $|b|>1$ having overestimated distances as adopted in ATNFPC. About 75% of 422 PSRs in ATNFPC have V_{trans} values below the average 265.7 km/s value. Although the number of PSRs with overestimated distances is relatively

small, they still cause the average speed value to be overestimated. Average space velocity of PSRs depends on the kick (asymmetry of the explosion), regardless of where the PSR was born (Yazgan et al. 2007; Katsuda et al. 2018). According to Allakhverdiev et al. (1997) and Hansen & Phinney (1997) the average space velocity of pulsars is 250-300 km/s. Considering that young pulsars ($\tau < 8 \times 10^5$ yr) must be located in or close to the star formation regions (molecular clouds, HI clouds, giant HII regions, SNRs, OB associations and open clusters) within the Galactic arms and the references given above, the average space velocity of pulsars must be about 300-350 km/s.

While constructing distance-DM relations, both characteristic age and average space velocity of pulsars (300-350 km/s) are taken into account as discussed in previous two paragraphs. Young pulsars whose $\tau < 8 \times 10^5$ yr are considered to be inside (or close to) the star formation regions (Galactic arms). The distance and the thickness of the Galactic arms are taken into account as criteria while determining distance-DM relations. Older pulsars ($\tau > 10^7$ years) can be located within Galactic arms, in between them or far away from them unless their space velocity is too small, so that the characteristic age is not a valid criterion for such pulsars in general.

There must be a correlation between the distribution of the HII regions, SNRs, OB associations and the Galactic distribution of free electrons in the vicinity of the Galactic plane. Their densities must also be correlated which is harder to show due to the lack of necessary observational data. Such correlations must be stronger at smaller distances and when considering only the Galactic arm regions. At large distances, the correlations must become weaker because of the presence of low density plasma between the arms. At larger distances from the Galactic plane, the free electron distribution must become more uniform with a decrease in its average value. Because of this fact, pulsars at larger Galactic latitudes must be located at relatively larger distances as compared to the pulsars at smaller latitudes with similar DM values at the same longitudes. The pulsars with large τ and/or the ones in the longitude intervals of the deviated arm regions must be considered separately.

The plasma regions in the Galactic bulge is not well known as compared to the plasma in arms nearer to the Sun, but their contribution to the values of DM can be more important than the plasma in the arms as seen in the case of the largest DM pulsar (SGR J1745-29).

The location, thickness and scale height of each Galactic arm are taken into account in adopting distances for the pulsars located at or close to the Galactic plane. For this, we assumed that the average value of the free electron number density increases as the line of sight passes through each arm as a function of distance for the pulsars in the same longitude and latitude intervals.

When adopting distances for pulsars in each solid angle interval (these groups of pulsars are given in the next section) independent distance measurements for them (like trigonometric parallax and associations with SNRs or stellar clusters) are also taken into consideration. Using the results of such measurements and making comparisons between pulsars in each group data lead to improved values of both distance and uncertainty in distance. The data used are mainly ℓ , b , DM, τ and also some of the other data displayed in the text of the next section and in Tables 1–A20). In these tables, data from ATNFPC and the ones adopted and calculated in this study are shown in separate columns.

3 RADIO PULSAR GROUPS IN DIFFERENT SOLID ANGLE INTERVALS IN THE FIRST QUADRANT

Below, some basic information and observational results for groups of Galactic radio pulsars in different solid angle intervals, covering the first quadrant of the Galaxy, are presented. Luminosity comparisons between radio pulsars and the Crab pulsar which is taken as a reference, are done using the measured flux at 1400 MHz to put a limit on the distance unless otherwise is stated. The measured transverse speeds (V_{trans}) of pulsars displayed in the ATNFPC are also presented.

3.1 $358^\circ < \ell < 2^\circ$; $-2^\circ < b < 2^\circ$

There are 29 radio pulsars in these Galactic central directions including some of the largest DM pulsars. Nine of the pulsars are young ($\tau < 8 \times 10^5$ yr) (see Table 1) that each of them must be located at or close to one of the Galactic arms or at the Galactic bulge.

One of the young pulsars in this group is the magnetar SGR J1745-29 with the largest DM (1778 pc/cm^3) among all the observed pulsars up to date. The magnetar's LOS passes through the HII region G359.964-00.101 with unknown distance (Anderson et al. 2014) and possibly through low-density parts (i.e. unobserved) of several other HII regions. SGR J1745-29 is probably located close to the Galactic center with its direction passing through Sgr A. It has also the largest RM measured up to date suggesting a location close to the Galactic center. Since SGR J1745-29 is only 3400 years old, it is also possible that this pulsar is located at a Galactic arm beyond the center considering its extremely large DM and the small number of RM measurements for pulsars to make conclusive comparisons. The magnetar has $V_{trans}=251.023 \text{ km/s}$ at $d=8.3 \text{ kpc}$ (ATNFPC), therefore if it is located at a distant arm beyond the center, its speed can be about about 2 times larger than the average speed of pulsars.

Eight of the 29 pulsars in this group have $DM > 800 \text{ pc/cm}^3$ (see Table 1) strongly suggesting the presence of dense plasma at the Galactic central regions. There is no observed pulsar with DM in the range $600 \text{ pc/cm}^3 < DM < 800 \text{ pc/cm}^3$ possibly corresponding to the interval between the Norma arm and the Galactic central region.

Young pulsar J1745-3040 ($\ell=358.553^\circ$, $b=-0.963^\circ$, $DM=88.373 \text{ pc/cm}^3$, $d=2.343 \text{ kpc}$ (YMW17), $\tau = 5.46 \times 10^5$ yr) is located at Sagittarius arm. It has $V_{trans}=46.78 \text{ km/s}$ at $d=0.2 \text{ kpc}$ (0.1-1.3 kpc, kinematic) according to ATNFPC. The speed of this pulsar is comparable to the average value at our adopted distance. Very young pulsar J1740-3015 ($\ell=358.294^\circ$, $b=0.238^\circ$, $DM=151.96 \text{ pc/cm}^3$, $d=2.944 \text{ kpc}$ (YMW17), $\tau = 2.06 \times 10^4$ yr) is located at Scutum arm. For this pulsar, 0.4 kpc (0.1-2.1 kpc, kinematic) is adopted in ATNFPC. J1752-2806 ($\ell=1.54^\circ$, $b=-0.961^\circ$, $DM=50.372 \text{ pc/cm}^3$, $d=1.335 \text{ kpc}$ (YMW17), $\tau = 1.1 \times 10^6$ yr) is probably at or close to Sagittarius arm, which has the adopted distance of 0.2 kpc (0.1-1.3 kpc, kinematic) in ATNFPC. There is no Local arm source in or close to the directions of these pulsars. If such very small distances (0.2-0.4 kpc) were correct, the average free electron density in the nearby region of the Sun would have been very large. herefore, the distances adopted in ATNFPC for these three pulsars based on the kinematic measurements listed in YMW17 model, must have an order of magnitude underestimated values.

RM values of J1752-2806 and J1745-3040 are both positive and similar in magnitude (see Table 1). Considering also their DM values, these two pulsars must be located in or close to the Sagittarius arm.

Pulsar J1752-2806 ($d=1.1-1.5 \text{ kpc}$) has a larger upper limit on the distance (taking the Crab pulsar as a reference) at 1400 MHz as

compared to 400 MHz which is an exceptional case. This pulsar may have a luminosity similar to that of Crab.

Young pulsar J1747-2958 ($\ell = 359.305^\circ$, $b = -0.841^\circ$, $DM = 101.5 \text{ pc/cm}^3$, $d = 2.5$ (ATNFPC) kpc, $\tau = 2.55 \times 10^4$ yr) is possibly associated with PWN G359.23-0.82 ($d < 3 \text{ kpc}$, Uchida et al. 1992); ($d = 2 \text{ kpc}$ Camilo et al. 2002); ($d < 5.5 \text{ kpc}$ (HI) Camilo et al. 2002); ($d = 4.8 \pm 0.8 \text{ kpc}$ (X-ray) Abdo et al. 2013) and located in the direction of the HII region G359.50-0.60 ($d = 1.5 \pm 0.2 \text{ kpc}$, Hou et al. (2009) with a lateral separation of only 8 pc.

Pulsars J1739-2903, J1740-3015, J1739-3023 and J1738-2955 have negative RM values ranging from -74 ± 18 to -236 ± 18 (see Table 1). Together with their DM values and considering the fact that all of them are young, they must be located within the Scutum arm. Pulsar J1741-2945 has a direction close to the directions of J1738-2955, J1739-3023 and J1740-3015 with a significantly larger DM. Therefore, the line of sight of this pulsar must pass through at least some part of the Norma arm as well and it may even be located within this arm.

Pulsars J1736-2843 and J1741-2719 have the largest latitudes in this group (see Table 1). Based on their DM values, the lines of sight of these pulsars are possibly not passing through the Scutum and the Norma arms. Their τ values are not small either, making the uncertainties in their distances larger.

Pulsars J1749-3002 ($b = -1.244^\circ$) and J1752-2821 ($b = -0.976^\circ$) have DM values comparable to each other (see Table 1). Model dependent and adopted distances (which are the same for each of them) for these two pulsars given in ATNFPC are 12.7 kpc and 5.4 kpc, respectively, with a distance ratio of about 2.4. If the latitude of J1752-2821 were even slightly smaller making its $b < -1^\circ$, the distance of this pulsar would be at least twice the value given in ATNFPC according to YMW17 model. These two pulsars must probably be located at similar distances.

There is the giant molecular cloud Sagittarius (Sgr) B2 ($\ell=0.67$, $b = -0.03$, $d = 7-8.6 \text{ kpc}$ Reid et al. 2009, 2014) possibly located close to the Galactic center. There are 451 HII regions in $\Delta\ell = \Delta b = 0^\circ \pm 2^\circ$ intervals around the Galactic center direction (Anderson et al. 2014). Distance measurements are available only for 17 of the HII regions locating all of them at 8 kpc in the intervals $\Delta\ell = 358.53^\circ - 358.95^\circ$ and $\Delta b = -0.116^\circ - 0.085^\circ$. None of the pulsars in this group has a LOS passing through any one of these HII regions.

Based on our adopted distances, J1749-3002 must be more luminous than the Crab pulsar by a factor of 2.8-4.8, while J1741-3016 and J1746-2850 must be more luminous or comparable to the Crab. J1747-2802, J1740-3015 and J1748-3009 may be comparable to and J1745-3040 must be comparable to or less luminous than the Crab pulsar (see Table 1 and Figure 1).

3.2 $2^\circ < \ell < 6^\circ$; $-2^\circ < b < 2^\circ$

Out of the 30 pulsars in this group, 9 are young ($\tau < 8 \times 10^5$ yr), though it must be noted that 4 of the pulsars have unknown τ (see Table A1). The solid angle intersects the Sagittarius, Scutum and Norma arms as well as the Galactic bulge and unknown possible arms beyond the bulge.

There is a Scutum arm source (G5.88-0.39) located at $d = 2.82 - 3.18 \text{ kpc}$ from parallax measurements (Sato et al. 2014; Reid et al. 2014, 2019).

The young pulsar J1801-2451 ($\ell=5.254^\circ$, $b=-0.882^\circ$, $DM=291.55 \text{ pc/cm}^3$, $d=4.5 \text{ kpc}$, $\tau = 1.55 \times 10^4$ yr, see Table A1) has $V_{trans}=199.15 \text{ km/s}$ at $d=3.803 \text{ kpc}$ (ATNFPC) and $z=-69 \text{ pc}$ at $d=4.5 \text{ kpc}$. There may be a deviation of the SFR from the Galactic plane in the direction of this pulsar at about $d=4-5 \text{ kpc}$ as J1801-2451

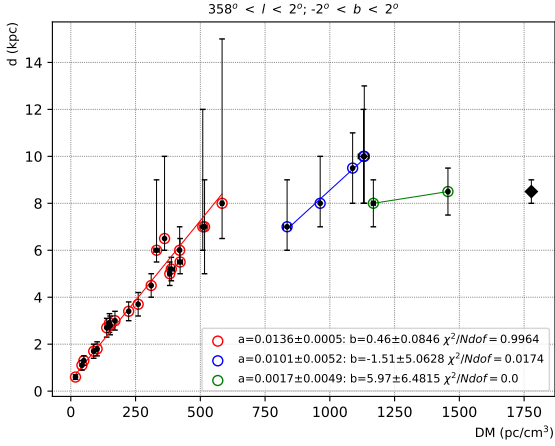


Figure 1. Distance-DM relations for radio pulsars in the solid angle interval $358^\circ < \ell < 2^\circ$; $-2^\circ < b < 2^\circ$. The data are fit to linear functions (shown in red, blue and green) with slopes a , and intercepts b .

Table 1. Radio pulsars in the solid angle interval $358^\circ < \ell < 2^\circ$; $-2^\circ < b < 2^\circ$ with measured DM. In the first column J-Name of the pulsar is given. The second and third columns are galactic latitude (ℓ) and longitude (b) of the pulsar in degrees. The fourth and fifth columns are dispersion measure (DM) values and their error in pc/cm^3 . The sixth and seventh columns are rotation measure (RM) values and their error in rad/m^2 . The eighth column is the characteristic ages (τ) of the pulsars in Myr. The ninth column is the ratio of rotation measure to dispersion measure (RM/DM). The tenth and eleventh columns are the adopted distances (d) and their error in kpc. The twelfth column is the Crab limit for the distance (d_{Crab}) in kpc. The thirteenth column is the distance to the Galactic plane (z) calculated from the adopted distance in pc. The symbol \dagger indicates the Crab (S400) luminosity limit.

PSR	Data from ATNFPC							Adopted and Calculated Data in this Study				
	ℓ degree	b degree	DM pc/cm^3	err pc/cm^3	RM rad/m^2	err rad/m^2	τ Myr	RM/DM	d kpc	err kpc	d_{Crab} kpc	z pc
J1753-28	0.887	-1.377	18	± 0.9	-	-	-	-	0.6	± 0.1	-	-14
J1751-2857	0.646	-1.124	42.84	± 0.03	-	-	5530	-	1.1	± 0.2	31	-22
J1752-2806	1.154	-0.961	52.72	± 0.08	96	± 0.2	1.1	1.9	1.3	± 0.2	14 \dagger , 1.08	-22
J1745-3040	358.553	-0.963	88.373	± 0.004	101	± 7.0	0.546	1.1	1.7	± 0.3	5.8 \dagger , 1.6	-29
J1747-2958	359.305	-0.841	101.5	± 1.6	-	-	0.0255	-	1.8	± 0.3	15	-26
J1739-2903	359.206	1.064	138.55	± 0.02	-236	± 18	0.65	-1.7	2.7	± 0.4	4	50
J1741-2733	0.636	1.582	149.2	± 1.7	-89.6	± 5.1	95.9	-0.6	2.9	± 0.4	6	80
J1740-3015	358.294	0.238	151.96	± 0.01	-168	± 0.7	0.0206	-1.1	2.8	± 0.4	9.5 \dagger , 2.5	12
J1739-3023	358.085	0.336	170.5	± 0.1	-74	± 18	0.159	-0.4	3	± 0.4	7	18
J1738-2955	358.378	0.724	223.4	± 0.6	-200	± 20	0.0857	-0.9	3.4	± 0.4	15	43
J1751-2737	1.761	-0.376	260	± 0.1	-	-	-	-	3.7	± 0.5	-	-24
J1741-2945	358.798	0.38	310.3	± 1.2	-531.1	± 9.1	5.58	-1.7	4.5	± 0.5	10	30
J1736-2843	359.142	1.764	331	± 10	-491.3	± 7.6	3.4	-1.5	6	± 3.0 , -0.5	11	246
J1741-2719	0.907	1.604	361.9	± 0.4	-	-	68.2	-	6.5	± 3.5 , -0.5	17	252
J1741-3016	358.346	0.13	382	± 6	-449.9	± 3.4	3.34	-1.2	5	± 0.5	5	11
J1750-28	0.663	-0.737	388	± 12	-	-	3.56	-	5.2	± 0.5	25	-67
J1748-3009	359.272	-1.147	420.2	± 0.01	-	-	-	-	6	± 1.0 , -0.5	6	-120
J1746-27	0.971	-0.494	422	± 9	-	-	-	-	5.5	± 1.0 , -0.5	15	47
J1749-3002	359.459	-1.244	509.4	± 0.3	-290	± 3.0	1.23	-0.6	7	± 5.0 , -1.0	13.2 \dagger , 3.7	-217
J1752-2821	1.267	-0.976	516.3	± 1.3	-	-	2.93	-	7	± 5.0 , -1.0	13	-170
J1748-30	359.117	-1.141	584	± 5	-	-	-	-	8	± 7.0 , -1.5	19	-239
J1747-2802	0.971	0.121	835	± 14	421	± 26	18.6	0.5	7	± 2.0 , -1.0	11	15
J1746-2850	0.134	-0.044	962.7	± 0.7	-	-	0.0127	-	8	± 2.0 , -1.0	8	-6
J1745-2910	359.763	-1.147	1088	± 0.1	-	-	-	-	9.5	± 1.5	-	-9
J1745-2912	359.788	-0.175	1230	± 20	-535	± 110	-	-0.5	10	± 2.0	-	-31
J1747-2809	0.869	0.076	1133	$\text{pm}3$	-	-	0.00531	-	10	± 3.0 , -2.0	-	-13
J1746-2856	0.126	-0.233	1168	± 7	13253	± 53	1.2	11.3	8	± 1.0	-	-33
J1746-2849	0.134	-0.03	1456	± 3	10104	± 100	1.84	6.9	8.5	± 1.0	12	-4
J1745-2900	359.944	-0.047	1778	± 3	-66080	± 24	0.0034	-37.2	8.5	± 0.5	-	-7

is possibly connected to SNR G5.27-0.9 ($d=5$ kpc (proper motion) Thorsett et al. 2002; Guseinov et al. 2003b). PSR – SNR G5.4-1.2 connection is established in Frail & Kulkarni (1991) ($d>4.3$ kpc Frail et al. 1994, $d \sim 5$ kpc Caswell et al. 1987, $d=4.5$ kpc Guseinov et al. 2003b, $d>4.3$ kpc (HI absorption suggests) Green 2019; Thorsett et al. 2002).

Pulsar J1748-2446A ($\ell=3.836^\circ$, $b=1.696^\circ$, $\text{DM}=242.15$ pc/cm^3 , $d=5$ kpc, τ is unknown, (see Table A1)) is a member of the globular cluster Ter 5 including 42 pulsars none of which has a measured τ and this globular cluster has a large uncertainty in its distance measurement ($d=4.6\text{--}10.3$ kpc Harris 1996; Cohn et al. 2002; Ortolani et al.

1996, 2001, 2007; Ferraro et al. 2009; Kong et al. 2010; Baumgardt et al. 2019; Valenti et al. 2007).

Five of the pulsars in this group may be more luminous than the Crab pulsar. See Figure A1 for distance-DM relation for this solid angle interval.

3.3 $6^\circ < \ell < 10^\circ$; $-2^\circ < b < 2^\circ$

There are 26 pulsars, 7 of which are young ($\tau < 8 \times 10^5$ yr, see Table A2). The solid angle intersects the Sagittarius, Scutum and Norma arms, possibly also intersecting the Perseus arm and the distant parts of the Sagittarius and Scutum arms beyond the Galactic central region.

There is a Norma arm source (Reid et al. 2014, 2019) in this interval: G9.62+0.19 ($d=4.6\text{--}5.8$ kpc Sanna et al. 2009).

PSR J1756-2251 ($d=2.1$ kpc) has $V_{\text{trans}}=8.38$ km/s at $d=0.73$ kpc (ATNFPC) (0.49-1.33 kpc, parallax (Yao et al. 2017)) and PSR J1802-2124 ($d=2.5$ kpc) has $V_{\text{trans}}=17.564$ km/s at $d=0.76$ kpc (ATNFPC). For pulsars J1753-2240 ($d=2.6$ kpc) and J1759-2205 ($d=2.9$ kpc), the ATNFPC adopted distances are 3.23 and 3.26 kpc, respectively. Therefore, the adopted distances in ATNFPC for pulsars J1756-2251 and J1802-2124 are probably underestimated values. The actual speeds of these pulsars must then be not so small.

Pulsar J1803-2137 has $V_{\text{trans}}=392.261$ km/s at $d=4.4$ kpc (ATNFPC). The actual distance of this pulsar may be 1-2 kpc smaller than the value adopted in ATNFPC, making its speed more comparable to the average pulsar speed.

One of the young pulsars is J1801-2304 ($\ell=6.837^\circ$, $b=-0.066^\circ$, $\text{DM}=1073.9$ pc/cm^3 , $d=13.5$ kpc, $\tau=5.83 \times 10^4$ yr, see Table A2) in the direction of the SNR W28 (G6.4-0.1) ($d=2.5$ kpc (Guseinov et al. 2003b), $d=1.9$ kpc (HI absorption) (Green 2019; Velázquez et al. 2002) and G7.0-0.1 ($d=9.5$ kpc (Guseinov et al. 2003b)). As the DM value of the pulsar is too large, a physical connection to SNR W28 is unlikely, so it may simply be a chance projection. A physical connection to SNR G7.0-0.1 considering the uncertainties in the distances is not ruled out but it is not very probable. Considering its position and the large DM, this young pulsar is probably related to a distant unobserved SNR beyond the Galactic central region.

Six of the pulsars in this group may be more luminous than the Crab pulsar at 1400 MHz (J1803-2137, J1812-2102, J1808-2057, J1759-2302, J1805-2032, J1801-2304) None of them are more luminous than the Crab pulsar at 400 MHz according to our adopted distances.

3.4 $10^\circ < \ell < 14^\circ$; $-2^\circ < b < 2^\circ$

There are 27 pulsars in this group, from which 6 are young ($\tau < 8 \times 10^5$ yr) (see Table A3). The solid angle intersects the Sagittarius, Scutum, Norma, Perseus and Cygnus arms as well as the outer parts of the Galactic bulge region. Two of the young pulsars, J1809-1943 ($\ell=10.727^\circ$, $b=-0.158^\circ$, $\text{DM}=178$ pc/cm^3 , $d=3$ kpc, $\tau=3.1 \times 10^4$ yr) and J1809-1917 ($\ell=11.094^\circ$, $b=0.08^\circ$, $\text{DM}=197.1$ pc/cm^3 , $d=3.3$ kpc, $\tau=5.13 \times 10^4$ yr), are located at the Scutum arm (see Table A3). The other young pulsars are probably located beyond the Norma arm.

There is a Sagittarius arm source (Reid et al. 2014, 2019; Wu et al. 2014) in this interval: G11.49-1.48 ($d=1.2\text{--}1.3$ kpc, arm offset = 120 – 220 pc). There are also several Scutum arm sources (Reid et al. 2014, 2019): G11.91-0.61 ($d=3.05\text{--}3.76$ kpc (Sato et al. 2014)); G12.68-0.18 ($d=2.25\text{--}2.57$ kpc (Immer et al. 2013)); G12.8-0.2 ($d=2.64\text{--}3.27$ kpc (Immer et al. 2013)); G12.88+0.48 (IRAS 18089-1732) ($d=2.27\text{--}2.78$ kpc (Immer et al. 2013)); G12.9-0.24 ($d=2.31\text{--}2.61$ kpc (Immer et al. 2013)); G12.9-0.26 ($d=2.34\text{--}2.75$

kpc (Immer et al. 2013)); G13.87+0.28 ($d = 3.6 - 4.35$ kpc (Sato et al. 2014)). Two sources located at the possible 3-kpc arm and a source at a 'connecting arm' are (Reid et al. 2014, 2019; Sanna et al. 2014): G10.62-0.38 (W31) ($d = 4.52 - 5.46$ kpc); G12.02-0.03 ($d = 8.77 - 10.2$ kpc) and G10.47+0.02 ($d = 8 - 9.2$ kpc).

J1806-1920 is more luminous than the Crab pulsar by a factor of 1.4-5.2 times and J1809- is at least as luminous as Crab. J1811-1736 and J1814-1744 has a luminosity comparable to that of Crab, whereas J1801-1855 and J1811-1835 may be at most as luminous as the Crab pulsar.

Distance for J1809-1943 from parallax measurements is given as $2.5^{+0.4}_{-0.3}$ kpc in Ding et al. (2020). Our adopted distance ($3\text{kpc} \pm 0.3$ (see Table A3 and Figure A3)) for the pulsar is in agreement with the parallax distance.

3.5 $14^\circ < \ell < 18^\circ$; $-2^\circ < b < 2^\circ$

Only five of the 28 pulsars in this group are young ($\tau < 8 \times 10^5$ yr) (see Table A4). This interval intersects the Sagittarius (twice), Scutum (twice) and Norma arms as well as the Galactic bulge region. The young pulsars are located at or close to these arms and the Galactic bulge. It is possible that J1821-1419 may be located at a distant arm (Perseus?) beyond far-Sagittarius.

The Sagittarius arm sources (Reid et al. 2014, 2019; Wu et al. 2014) in this interval are: G14.33-0.64 ($d = 1.01 - 1.26$ kpc, arm offset = 200 – 440 pc Sato et al. 2010); G14.63-0.57 ($d = 1.77 - 1.9$ kpc, arm offset = -400 – -260 pc); G15.03-0.67 (M 17) ($d = 1.86 - 2.11$ kpc, arm offset = -570 – -330 pc Xu et al. 2011). There is only one Scutum arm source Reid et al. (2014, 2019); Sato et al. (2014): G16.58-0.05 ($d = 3.31 - 3.9$ kpc).

Although, the solid angle cuts through different parts of several arms, the number of young pulsars is relatively low, possibly due to the fact that the intersection depths through the arms are small.

Pulsars J1818-1422, J1818-1519 and J1820-1346 are more luminous than the Crab pulsar by a factor of 3.9-13.1, 2-7 and 1.7-5.9 times, respectively. J1819-1408 is probably at least as luminous as the Crab pulsar. Pulsars J1818-1541, J1817-1511, J1820-1529, J1825-1446, J1821-1419, J1822-1400, J1823-1347 may have luminosity comparable to the Crab pulsar's based on their adopted distances.

Pulsars J1818-1519 ($\ell=15.55^\circ$, $b=0.192^\circ$, $DM=845$ pc/cm³, $d=10.5$ kpc, $\tau = 3.63 \times 10^6$ yr) and J1818-1422 ($\ell=16.405^\circ$, $b=0.61^\circ$, $DM=622$ pc/cm³, $d=8.1$ kpc, $\tau = 2.27 \times 10^6$ yr) (see Table A4) are most probably more luminous than the Crab pulsar based on our adopted distances.

3.6 $18^\circ < \ell < 22^\circ$; $-2^\circ < b < 2^\circ$

In this group, 32 pulsars are included 9 of which are young ($\tau < 8 \times 10^5$ yr) (see Table A5). The youngest one, J1833-1034 ($\ell=21.501^\circ$, $b=-0.885^\circ$, $DM=169.5$ pc/cm³, $d=3.5$ kpc, $\tau = 4.85 \times 10^3$ yr) (see Table A5)), is probably physically connected to the C-type SNR G21.5-0.9 ($d(\text{kinematic}) \sim 4.8$ kpc Tian & Leahy 2008, $d = 4.3$ kpc, Lee et al. 2019 and references therein, $d = 4.4^{+0.2}_{-0.2}$ (HI absorption) Ranasinghe & Leahy 2018, $d > 2.9$ kpc (optical) Shan et al. 2018). This pulsar is probably located at a slightly deviated part ($z = -54$ pc at 3.5 kpc (see Table A5)) of the Scutum arm in a dense star formation region in between and possibly connected to the Sagittarius and the Norma arms. The other young pulsars of the group are located at or close to these three arms (J1822-1252 may be at Perseus or far-Sagittarius).

J1828-1101 is more luminous than the Crab pulsar up to a factor

of 4.7. J1823-1115, J1824-1118, J1827-0958 and J1832-1021 are probably more luminous but may be comparable in the limit, whereas J1822-1252, J1823-1126, J1831-1223 and J1833-1055 are at most as luminous as the Crab pulsar.

3.7 $22^\circ < \ell < 26^\circ$; $-2^\circ < b < 2^\circ$

This solid angle intersects the Sagittarius and Scutum arms twice, possibly also intersecting the edge of the Norma arm at about $\ell=22^\circ$ which is possibly separated from the Scutum at most by 1 kpc. As large parts of star formation regions are included within this interval, 16 young pulsars are present in the group out of a total of 41 pulsars (see Table A6). The young pulsars ($\tau < 8 \times 10^5$ yr) are located mostly at or close to the Scutum arm, while several of them are probably related to the Norma or the Sagittarius arms.

There is one Scutum arm source and three Norma arm sources (Sato et al. 2014; Reid et al. 2014, 2019; Brunthaler et al. 2009): G25.7+0.04 ($d = 7.87 - 14.49$ kpc) and G23.0-0.41 ($d = 4.26 - 4.98$ kpc); G23.44-0.18 ($d = 4.95 - 7.25$ kpc); G23.7-0.19 ($d = 5.4 - 7.3$ kpc). High-mass Star Forming Region (HMSFR) source G23.65-0.12 ($d = 2.84 - 3.65$ kpc Reid et al. 2014, 2019; Bartkiewicz et al. 2008) may be a Scutum arm source or in between the Scutum and the Sagittarius.

J1833-0827, a young radio pulsar ($\tau = 1.47 \times 10^5$ yr), is probably more luminous than the Crab pulsar up to a factor of 3.5 based on our adopted distance. J1836-1008 ($\tau = 7.56 \times 10^5$ yr), J1827-0750 ($\tau = 2.77 \times 10^6$ yr) and J1840-0809 ($\tau = 6.44 \times 10^6$ yr) (see Table A6) are possibly more luminous than the Crab pulsar. J1832-0827, J1840-0753, J1832-0644, J1835-0643, J1837-0653, J1839-0643 and J1840-0643 have luminosity possibly comparable to that of Crab. J1834-0633 and J1834-0602 are probably less luminous than the Crab pulsar but may possibly be comparable in the limit.

3.8 $26^\circ < \ell < 30^\circ$; $-2^\circ < b < 2^\circ$

There are 50 pulsars in this interval. About 1/3 of these pulsars are young ($\tau < 8 \times 10^5$ yr) (see Table A7) as this interval intersects the Scutum longitudinally including a large number of HII regions as well as molecular clouds. All but three of the young pulsars are at or close to the Scutum arm; J1849-0317 is definitely at the Sagittarius arm, J1844-0538 is at either Scutum or a distant part of Sagittarius, and J1838-0453 is either at Scutum, far-Sagittarius or even far-Perseus.

In this interval, the Scutum arm sources are (Reid et al. 2014, 2019): G27.36-0.16 ($d = 5.99 - 12.05$ kpc Sato et al. 2014); G28.86+0.06 ($d = 6.54 - 8.55$ kpc); G29.86-0.04 ($d = 5.52 - 7.09$ kpc Sato et al. 2014); G29.95-0.01 (W 43S) ($d = 4.78 - 5.84$ kpc Sato et al. 2014).

Young and distant pulsar J1838-0453 ($\ell=27.07^\circ$, $b=0.708^\circ$, $DM=617.2$ pc/cm³, $d=10.5$ kpc, $\tau = 5.19 \times 10^4$ yr) has $z=130$ pc (see Table A7), probably located at a deviated part of an SFR.

This group includes several possibly luminous pulsars as compared to the Crab pulsar: J1844-0538 may be up to about 5 times as luminous as the Crab pulsar. J1842-0612, J1838-0453 and J1848-0511 are probably less luminous than Crab pulsar but may be comparable in the limit. J1843-0355 can be as luminous, less luminous or up to 3 times more luminous than the Crab pulsar within distance uncertainties.

3.9 $30^\circ < \ell < 34^\circ$; $-2^\circ < b < 2^\circ$

Seven out of 31 pulsars in this group are young ($\tau < 8 \times 10^5$ yr) (see Table A8) and probably located at or close to the Scutum arm.

The Scutum arm sources are (Reid et al. 2014, 2019; Sato et al. 2014; Zhang et al. 2014): G31.28+0.06 ($d = 3.66 - 5.12$ kpc); G31.58+0.07 (W 43Main) ($d = 4.27 - 5.75$ kpc); G32.04+0.05 ($d = 4.97 - 5.4$ kpc). HMSFR source G33.64-0.22 ($d = 5.88 - 7.35$ kpc Reid et al. 2014, 2019) is probably a Scutum arm source (there is longitudinal intersection of the LOS through a large portion of the Scutum arm).

PSR J1844+00 is up to an order of magnitude more luminous than the Crab pulsar. Pulsars J1852+0031, J1850-0026 and J1848-0123 are possibly 1.4-2.8, 1.4-2.7 and 1.3-2.4 times as luminous as the Crab pulsar, respectively.

3.10 $34^\circ < \ell < 38^\circ$; $-2^\circ < b < 2^\circ$

Thirteen of the 47 pulsars in this group are young ($\tau < 8 \times 10^5$ yr) (see Table A9). Young pulsar J1856+0113 ($\ell=34.56^\circ$, $b = -0.497^\circ$, $DM=96.74$ pc/cm³, $d=2.8$ kpc, $\tau = 2.03 \times 10^4$ yr) is physically connected to the C-type SNR W44 (G34.7-0.4, HI measurements indicates a distance of about 3 kpc (Radhakrishnan et al. 1972; Green 2019), ($d = 2.8$ kpc Guseinov et al. 2003b; Lee et al. 2019 and references therein, $d = 3^{+0.3}_{-0.3}$ kpc (HI absorption) Ranasinghe & Leahy 2018, $d=2.1 \pm 0.2$ kpc (optical) Shan et al. 2018). This pulsar-SNR pair is located at the Sagittarius arm which includes sources at similar distances. The other young pulsars of the group are probably located at or close to either the Sagittarius or the Scutum arms. Young and distant pulsar J1857+0210 ($\ell=35.586^\circ$, $b = -0.393^\circ$, $DM=783$ pc/cm³, $d=11$ kpc, $\tau = 7.12 \times 10^5$ yr, see Table A9) may possibly be located close to the Perseus arm instead of the Sagittarius arm.

The Sagittarius arm sources are (Reid et al. 2014; Wu et al. 2014): G34.39+0.22 ($d = 1.45 - 1.69$ kpc, arm offset = 160 – 320 pc Kuroyama et al. 2011); G35.02+0.34 ($d = 2.12 - 2.56$ kpc, arm offset = -90 – -350 pc Reid et al. 2009); G35.19-0.74 ($d = 1.99 - 2.43$ kpc, arm offset = -20 – -260 pc Zhang et al. 2009); G35.2-1.73 ($d = 2.85 - 3.83$ kpc, arm offset = -490 – -930 pc Zhang et al. 2009); G37.43+1.51 ($d = 1.8 - 1.96$ kpc, arm offset = 70 – 150 pc Reid et al. 2009).

The Scutum and the Sagittarius arms are closer to each other in the approximate distance interval 4-8 kpc in these directions increasing the uncertainty of the young pulsar locations (Hou et al. 2009; Hou & Han 2014).

Young pulsar J1857+0210 should have a luminosity comparable to that of the Crab pulsar if it is located beyond but close to the Perseus arm, while the younger pulsar J1857+0212 in this direction, probably located at the Sagittarius arm, has 1.2-2.4 times the Crab pulsar's luminosity. Pulsars J1859+00 and J1903+0135 must be 2.9-8.2 and 2.3-4 times more luminous than the Crab pulsar, respectively. Pulsars J1859+00 and J1903+0135 must be 2.9-8.2 and 2.3-4 times more luminous than the Crab pulsar, respectively. J1901+0331 has luminosity 2.6-4.7 times the Crab pulsar's luminosity both at 400 MHz and 1400 MHz. J1855+0307, J1903+0327 and J1853+0505 may have luminosity comparable to or slightly less than that of the Crab pulsar. Luminous pulsar J1901+0331 has $V_{trans}=1511.36$ km/s at $d=7$ kpc (ATNFPC).

3.11 $38^\circ < \ell < 42^\circ$; $-2^\circ < b < 2^\circ$

This crowded group has 55 members including some of the pulsars with the smallest and the largest τ values. Fourteen of these pulsars

are young ($\tau < 8 \times 10^5$ yr) which are probably located at or close to the Sagittarius arm. Pulsar J1901+0459 ($\ell=38.49^\circ$, $b=0.087^\circ$, $DM=1108$ pc/cm³, $d=13.5$ kpc, $\tau = 8.86 \times 10^5$ yr, see Table A10) may be located at or close to the Perseus arm or the Cygnus arm.

Young pulsar J1855+0527 ($\ell=38.227^\circ$, $b = 1.642^\circ$, $DM=362$ pc/cm³, $d=7$ kpc, $\tau = 8.26 \times 10^4$ yr, see Table A10) is probably located at a deviated part of an SFR as its distance from the Galactic plane is 201 pc.

For recycled millisecond (ms) pulsars J1905+0400 ($P=3.8$ ms, $\tau=1.22 \times 10^{10}$ yr), J1904+0412 ($P=71$ ms, $\tau=1.02 \times 10^{10}$ yr), J1904+0451 ($P=6$ ms, $\tau=1.69 \times 10^{10}$ yr) and J1914+0659 ($P=18.5$ ms, $\tau=9.46 \times 10^9$ yr) (ATNFPC), the real ages are not related to their characteristic ages as such radio pulsars are formed after the X-ray binary phase in close binary systems (Bisnovaty-Kogan & Komberg 1976, 1974).

Although the number of pulsars is relatively large in this group, there is no known arm source in this interval.

J1901+0435 must be one order of magnitude more luminous than the Crab pulsar and J1906+0641 has luminosity 1.3-2.7 times larger than the Crab's. J1857+0526, J1907+0534, J1905+0600 and J1910+0534 may be as luminous as the Crab pulsar.

3.12 $42^\circ < \ell < 46^\circ$; $-2^\circ < b < 2^\circ$

The solid angle of this group cuts through the Sagittarius arm including a large number of HII regions and molecular clouds, also intersecting a small part of the Perseus arm and possibly the Cygnus arm. There are 11 young ($\tau < 8 \times 10^5$ yr) pulsars (see Table A11) all of which are most probably located at or close to the Sagittarius arm in large distance intervals. Two of the 40 pulsars in this group are probably located close to the Perseus arm: J1905+0902 ($\ell=42.555^\circ$, $b=1.056^\circ$, $DM=433.4$ pc/cm³, $d=11$ kpc, $\tau = 9.88 \times 10^5$ yr) and J1913+1145 ($\ell=45.92^\circ$, $b=0.476^\circ$, $DM=637$ pc/cm³, $d=11.5$ kpc, $\tau = 9.67 \times 10^5$ yr, see Table A11).

There are Sagittarius arm sources in this interval (Reid et al. 2014, 2019; Wu et al. 2014): G43.79-0.12 (OH 43.8-0.1) ($d = 5.84 - 6.21$ kpc, arm offset = -470 – -530 pc); G43.89-0.78 ($d = 7.09 - 9.9$ kpc, arm offset = -770 – 1210 pc); G45.07+0.13 ($d = 7.35 - 8.19$ kpc, arm offset = -10 – 290 pc); G45.45+0.05 ($d = 7.35 - 9.8$ kpc, arm offset = -380 – 1360 pc). There is only one Perseus arm source: G43.16+0.01 (W 49N) (Reid et al. 2014, 2019) ($d(\text{parallax}) = 10.42 - 11.9$ kpc (Zhang et al. 2013), $d(\text{kinematic}) = 10.43 - 11.28$ kpc (Choi et al. 2014)).

Dense plasma regions of the Sagittarius arm in this longitude interval are possibly located at: $\ell=42^\circ$, $d=1.7-5.4$ kpc, $d=8-8.9$ kpc; $\ell=43^\circ$, $d=1.7-3.6$ kpc, $d=4.8-5.4$ kpc, $d=8-8.9$ kpc; $\ell=44^\circ$, $d=1.7-2.7$ kpc, $d=8-8.5$ kpc; $\ell=45^\circ$, $d=1.7-2.2$ kpc, $d=4.8-4.9$ kpc, $d=6.6-8.5$ kpc; $\ell=46^\circ$, $d=1.7-2.2$ kpc, $d=6-7.6$ kpc (Anderson et al. 2014; Hou & Han 2014).

Young pulsar J1907+0918 ($\ell=43.024^\circ$, $b=0.73^\circ$, $DM=357.9$ pc/cm³, $d=8.5$ kpc, $\tau = 3.8 \times 10^4$ yr) with $z=108$ pc (see Table A11) is located at a deviated part of an SFR.

Pulsars J1916+0844, J1915+1009, J1920+1040 and J1913+1145 may have luminosity comparable to the Crab pulsar, while most of the others are definitely much less luminous than the Crab.

3.13 $46^\circ < \ell < 50^\circ$; $-2^\circ < b < 2^\circ$

This group includes 21 pulsars, three of which are young ($\tau < 8 \times 10^5$ yr) and four of which with unknown τ (see Table A12). The solid angle intersects Sagittarius (longitudinal) and Perseus arms. There is no known HMSFR up to about 5 kpc in these directions.

There are 41 HII regions with measured distance within this solid angle (Anderson et al. 2014): G046.495-00.241 and G049.589-00370 at about 3.8 kpc; 23 HII regions at about 5.3-5.8 kpc; G048.547-00.005 at about 9 kpc; 7 HII regions at about 10 kpc; G046.173+00.533 and G046.213+00.547 at about 11 kpc; G048.719+01.147, G049.408+00.332 and G049.420+00.320 at about 13 kpc; G046.948+00.371 at about 15 kpc; G047.094+00.492 and G047.100+00.479 at about 16 kpc. Only one of these HII regions coincides with the direction of a member of this group: HII region G046.792+00.284 in the LOS of young pulsar J1916+1225.

The Sagittarius arm sources in the interval are (Reid et al. 2014, 2019; Wu et al. 2014): G49.19-0.34 ($d = 4.98 - 5.47$ kpc, arm offset = $-50 - -90$ pc); G49.48-0.36 (W 51 IRS2) ($d = 3.75 - 8.06$ kpc, arm offset = $-860 - 740$ pc); G49.48-0.38 (W 51M) ($d = 5.12 - 5.71$ kpc, arm offset = $-60 - 0$ pc). There is one Perseus arm source (Reid et al. 2014, 2019): G48.6+0.02 ($d(\text{parallax}) = 10.2 - 11.36$ kpc Zhang et al. 2013, $d(\text{kinematic}) = 8.7 - 9.63$ kpc Choi et al. 2014).

3.14 $50^\circ < \ell < 54^\circ$; $-2^\circ < b < 2^\circ$

In this group, 9 of the 27 pulsars, 5 of which are young, have unknown τ (see Table A13). Relatively large number of pulsars with unmeasured \dot{P} (unknown τ) makes it more difficult to determine the locations and to make comparisons of their luminosity for the pulsars in this group.

Four of the 5 young ($\tau < 8 \times 10^5$ yr) pulsars belong to the Sagittarius arm: J1926+1648 ($\ell=51.859^\circ$, $b=0.063^\circ$, $DM=176.885$ pc/cm³, $d=4$ kpc, $\tau = 5.11 \times 10^5$ yr), J1928+1746 ($\ell=52.931^\circ$, $b=0.114^\circ$, $DM=176.68$ pc/cm³, $d=4$ kpc, $\tau = 8.26 \times 10^4$ yr), J1925+1720 ($\ell=52.179^\circ$, $b=0.59^\circ$, $DM=223.3$ pc/cm³, $d=5.3$ kpc, $\tau = 1.15 \times 10^5$ yr), J1922+1733 ($\ell=52.08^\circ$, $b=1.23^\circ$, $DM=238$ pc/cm³, $d=5.4$ kpc, $\tau = 2.8 \times 10^5$ yr). Pulsar J1924+1631 ($\ell=51.405^\circ$, $b=0.318^\circ$, $DM=518.5$ pc/cm³, $d=10$ kpc, $\tau = 1.28 \times 10^5$ yr), which has the largest DM among the young pulsars of this group, most probably belongs to the Perseus arm (see Table A13).

J1926+1648 has $V_{\text{trans}} = 463.064$ km/s at $d=6$ kpc ($d(\text{kinematic}) = 4-9$ kpc, (Yao et al. 2017)) as displayed in ATNFPC. The transverse speed is more comparable to the average space velocity of pulsars (about 300 km/s) at our adopted distance of 4 kpc (see Table A13 and Figure A13).

There is only one Sagittarius arm source (Reid et al. 2014, 2019): G52.1+1.04 (IRAS 19213+1723) ($d = 3.48 - 4.65$ kpc, arm offset = $50 - 210$ pc Wu et al. 2014, $d = 5.62 - 6.58$ kpc Wu et al. 2019).

All the pulsars with measured flux in this group are less luminous than the Crab pulsar.

3.15 $54^\circ < \ell < 58^\circ$; $-2^\circ < b < 2^\circ$

There are 19 pulsars in this group, four of which are young and four of them have unknown τ (see Table A14). Very young ($\tau=2890$ yr) pulsar J1930+1852 ($DM=308$ pc/cm³) connected to SNR G54.1+0.3 ($d=6^{+2.2}_{-1.5}$ kpc (Guseinov et al. 2003b), $d(\text{optical})=6.3^{+0.8}_{-0.7}$ kpc Shan et al. 2018; Green 2019, $d = 4.9^{+0.8}_{-0.8}$ (HI absorption) (Ranasinghe & Leahy 2018; Green 2019), $d=8.2$ kpc (association with CO) Lee et al. 2012; Green 2019), type is C? (i.e. possibly composite type SNR) in Green's catalogue (Green 2019)) is probably located at Sagittarius arm at 6.7 ± 0.5 kpc. The other three young pulsars (all with $\tau < 6.3 \times 10^4$ yr) must also belong to the Sagittarius. The four young pulsars have significantly different adopted distances (about 2.5, 4.5, 5.5 and 6.7 kpc) due to the fact that their LOSs intersect the Sagittarius arm longitudinally (see Table A14).

PSR J1939+2134 ($d(\text{parallax}) = 1.5^{+0.5}_{-0.3}$ (Reardon et al. 2016b), $d(\text{parallax}) > 3.23$, (Matthews et al. 2016)), $V_{\text{trans}}=6.755$ km/s ($d=3.5$ kpc (ATNFPC)) has the Crab limits $d_{\text{Crab}} < 3.1$ kpc (S400), $d_{\text{Crab}} < 2.1$ kpc (S1400). PSR J1939+2134 was the first ms pulsar observed (Backer et al. 1982), and it is currently the second fastest spinning pulsar known (Reardon et al. 2016b) with $V_{\text{radial}}=89.16$ km/s (Matthews et al. 2016) which is isolated due to the disruption during the core-collapse SN).

For the ms recycled pulsar J1939+2134, we adopted $d=1.5-2.5$ kpc (see Figure A14 and Table A14) making it slightly less luminous than the Crab pulsar at 400 MHz and comparable to the Crab at 1400 MHz. In ATNFPC, $d=3.5$ kpc is given as the adopted distance in which case this old (recycled) ms pulsar must be more luminous than the Crab at both 400 MHz and 1400 MHz. As the luminosity of old ms pulsars are mostly much less than the Crab pulsar, $d=3.5$ kpc is probably an overestimated value.

Young pulsar J1932+2220 ($\ell=57.356^\circ$, $b= 1.554^\circ$, $DM=219.2$ pc/cm³, $d=5.5$ kpc, $\tau = 3.98 \times 10^4$ yr (ATNFPC)) has $z=149$ pc, is probably located at a deviated part of a SF from the Galactic plane (see Table A14).

3.16 $58^\circ < \ell < 62^\circ$; $-2^\circ < b < 2^\circ$

Six of the 14 pulsars are young in this group with one unknown τ (see Table A15).

Young pulsar J1939+2449 ($\ell=60.174^\circ$, $b= 1.361^\circ$, $DM=142.88$ pc/cm³, $d=6$ kpc, $\tau = 5.6 \times 10^5$ yr) is probably located close to the far end of the Sagittarius arm in this direction. J1940+2245 ($\ell=58.629^\circ$, $b=0.127^\circ$, $DM=222.4$ pc/cm³, $d=8.2$ kpc, $\tau = 3.23 \times 10^5$ yr), J1940+2337 ($\ell=59.397^\circ$, $b= 0.529^\circ$, $DM=252.1$ pc/cm³, $d=8.8$ kpc, $\tau = 1.13 \times 10^5$ yr) and J1948+2333 ($\ell=60.214^\circ$, $b= -1.045^\circ$, $DM=198.2$ pc/cm³, $d=8.2$ kpc, $\tau = 6.17 \times 10^5$ yr) are at or close to the Perseus arm. Distant young pulsars J1934+2352 ($\ell=58.966^\circ$, $b= 1.814^\circ$, $DM=355.5$ pc/cm³, $d=14$ kpc, $\tau = 2.16 \times 10^4$ yr) and J1941+2525 ($\ell=61.037^\circ$, $b= 1.263^\circ$, $DM=314.4$ pc/cm³, $d=13$ kpc, $\tau = 2.27 \times 10^5$ yr) (see Table A14) may belong to the Outer or Outer+1 arm despite their large distances from the Galactic plane (about 440 pc and 290 pc, respectively) as the HMSFRs close to these directions have large positive offsets from the Galactic plane (Hou & Han 2014).

Although, the pulsars in this solid angle interval have large distances with respect to their DM values as compared to the previous groups, all of them are probably less luminous than the Crab pulsar.

There is one Local arm source (Reid et al. 2014, 2019): G59.78+0.06 ($d = 2.07 - 2.26$ kpc Xu et al. 2009).

3.17 $62^\circ < \ell < 66^\circ$; $-2^\circ < b < 2^\circ$

There are 9 pulsars in this group two of which are young (see Table A16). The two young pulsars of this group, J1948+2551 ($\ell=62.207^\circ$, $b= 0.131^\circ$, $DM=289.27$ pc/cm³, $d=8.7$ kpc, $\tau = 3.45 \times 10^5$ yr) and J1946+2611 ($\ell=62.321^\circ$, $b= 0.595^\circ$, $DM=165$ pc/cm³, $d=6.3$ kpc, $\tau = 3.14 \times 10^5$ yr), are probably located at the Perseus arm and close to the Sagittarius arm, respectively, though J1946+2611 may be close to the Perseus arm.

Proper motions of four of the pulsars in this solid angle interval were measured. For three of these pulsars, the distances we have adopted are in agreement with the adopted distances displayed in ATNFPC. J1955+2908 is an old ms pulsar ($P=6.133$ ms, $\dot{P}=2.97 \times 10^{-20}$, $\tau = 3.27 \times 10^9$ yr) which is most probably located at a smaller distance than the one adopted in ATNFPC ($d=6.3$ kpc) considering its DM

as compared to the other members of this group and the Crab limit on its distance ($d_{Crab} < 7.2$ kpc) together with its large τ value. The transverse speeds at our adopted distances are reasonable (100-300 km/s).

All the pulsars in this group are probably less luminous than the Crab pulsar. Pulsar J1948+2551's luminosity may be close to the Crab's, considering the uncertainty in its luminosity.

3.18 $66^\circ < \ell < 70^\circ$; $-2^\circ < b < 2^\circ$

At least four of the 11 pulsars in this interval are young (τ is unknown for 5 pulsars (see Table A17)) that they must be located at or close to the Perseus and the Sagittarius arms based on their DM values. Pulsar J2002+30 of unknown τ may also be young considering its small latitude ($b = -0.187^\circ$) and the possible distance interval (6-8 kpc) making it a member of the Perseus arm.

There is a Local arm source (Reid et al. 2014, 2019): G69.54-0.97 (ON 1) ($d = 2.39 - 2.54$ kpc) which is not related to the pulsars in this group.

Pulsar J2004+3137, which has the largest DM in this group, is more luminous than the Crab pulsar up to a factor of about 2.2. This pulsar has a high transverse speed (about 400 km/s at $d=7.8$ kpc) as compared to the average space velocity of pulsars. Pulsar J2002+3217 is possibly as luminous as the Crab within the distance uncertainties.

3.19 $70^\circ < \ell < 74^\circ$; $-2^\circ < b < 2^\circ$

There are 5 pulsars in this interval. The only young pulsar of this group, J2004+3429 ($\ell=71.425^\circ$, $b=1.571^\circ$, $DM=351$ pc/cm³, $d=12.5$ kpc, $\tau = 1.85 \times 10^4$ yr) (see Table A18), must be located in a HMSFR, probably within the Outer arm or the possible Outer+1 arm (see e.g. Hou & Han 2014 for the possible structures of distant arms in these directions). The distance of this very young pulsar from the Galactic plane is 288 pc $< z < 398$ pc, based on the large latitude of this pulsar together with its large distance. This does not prevent this pulsar to locate in a HMSFR within a Galactic arm as there are several giant molecular clouds (GMCs) at about 11.5-13.5 kpc with large positive offsets from the Galactic plane (Hou & Han 2014).

All the members of this group are less luminous than Crab pulsar, despite the fact that their adopted distances are large.

3.20 $74^\circ < \ell < 78^\circ$; $-2^\circ < b < 2^\circ$

There are four pulsars in the group, two of them are very young and one of them is young (see Table A19).

The Local arm sources are (Reid et al. 2014, 2019): G74.03-1.71 ($d = 1.55 - 1.63$ kpc Xu et al. (2013)); G75.76+0.33 ($d = 3.26 - 3.8$ kpc Xu et al. (2013)); G75.78+0.34 (ON 2N) ($d = 3.41 - 4.02$ kpc); G76.38-0.61 ($d = 1.22 - 1.39$ kpc Xu et al. (2013)). All these sources are foreground objects with respect to the pulsars in this interval. There is one Outer arm source: G75.29+1.32 ($d = 8.8 - 9.7$ kpc Sanna et al. 2012).

In the ATNFPC, $d(\text{kinematic, HI measurements})=1.8$ kpc is given as the adopted distance for the very young pulsar J2021+3651 ($\ell=75.222^\circ$, $b=0.111^\circ$, $DM=367.5$ pc/cm³, $d=11$ kpc, $\tau = 1.72 \times 10^4$ yr), which is a significantly underestimated value considering the large DM of this pulsar in this direction. PWN G75.2+0.1 is powered by J2021+3651 (Hessels et al. 2004). Abdo et al. (2013) give $d=6-12$ kpc for this pulsar. Kirichenko et al. (2015) give a distance of 1.8

^{+1.7}_{-1.4} kpc for J2021+3651 from X-ray and extinction-distance relation. Comparing the DM of this pulsar with the others in this interval and the neighbouring ones, also considering the possible location and structure of the Outer arm in this direction, we have adopted $d=10-12$ kpc for J2021+3651 (see Figure A19 and Table A19).

PSR J2022+3842 ($\ell=76.888^\circ$, $b=0.96^\circ$, $DM=429.1$ pc/cm³, $d=13$ kpc, $\tau = 8.94 \times 10^3$ yr, $z=218$ pc) is another very young pulsar in this interval which has the largest DM among the four pulsars. This pulsar is probably connected to the C-type SNR G76.9+1.0 ($d=10 \pm 3$ Arumugasamy et al. 2014; Arzoumanian et al. 2011, $d=12.6$ kpc Guseinov et al. 2003b). We have adopted $d=11-15$ kpc (see Figure A19 and Table A19) taking into account the large latitude and the large DM of the pulsar together with the large positive offsets of the GMCs from the Galactic plane close to this direction at large distances (Hou & Han 2014).

For the young pulsar J2030+3641 ($\ell=76.123^\circ$, $b= -1.438^\circ$, $DM=246$ pc/cm³, $d=9.5$ kpc, $\tau = 4.88 \times 10^5$ yr, $z=-238$ pc), Abdo et al. (2013) give $d=3 \pm 1$ kpc. As the latitude of this pulsar is relatively large and its DM is not so small to locate it at 3 kpc, we have adopted $d=8.7-11$ kpc (see Figure A19 and Table A19). Since this pulsar is below the Galactic plane, its transverse speed must be high at such large distances. Note that the adopted distance of J2030+3641 is 7 kpc in ATNFPC which leads to a similar conclusion.

All the three young pulsars of the group are possibly located at the Outer arm, though it may also be possible that J2030+3641 is closer to the Perseus arm and J2022+3842 is a member of the possible Outer+1 arm instead of the Outer arm.

Based on the Crab limit on their distances, three of the four pulsars should be less luminous than the Crab pulsar despite their large distances.

3.21 $78^\circ < \ell < 90^\circ$; $-2^\circ < b < 2^\circ$

$78^\circ < \ell < 82^\circ$; $-2^\circ < b < 2^\circ$

There is only one pulsar in this interval, namely J2032+4127 ($\ell=80.224^\circ$, $b=1.028^\circ$, $DM=114.67$ pc/cm³, $d=1.4-1.7$ kpc, $\tau = 2.01 \times 10^5$ yr) (see Table A20). This young pulsar is a member of the OB-association Cygnus OB2 at $d=1.4-1.7$ kpc (Lyne et al. 2015).

There are several Local arm sources in this interval (Reid et al. 2014, 2019): G78.88+0.7 (AFGL 2591) ($d = 3.23 - 3.45$ kpc Rygl et al. 2012); G79.73+0.99 (IRAS 20290+4052) ($d = 1.25 - 1.48$ kpc Rygl et al. 2012); G79.87+1.17 ($d = 1.55 - 1.69$ kpc Xu et al. (2013)); G80.79-1.92 (NML Cyg) ($d = 1.5 - 1.75$ kpc Zhang et al. 2012); G80.86+0.38 (DR 20) ($d = 1.38 - 1.55$ kpc Rygl et al. 2012); G81.75+0.59 (DR 21) ($d = 1.43 - 1.58$ kpc Rygl et al. 2012); G81.87+0.78 (W 75N) ($d = 1.23 - 1.37$ kpc Rygl et al. 2012). Therefore, young pulsar J2032+4127 must be a member of the Local arm. Note that the DM-based distance in YMW17 model is 4.62 kpc, though a distance of 1.33 kpc is adopted for this pulsar in ATNFPC.

$82^\circ < \ell < 86^\circ$; $-2^\circ < b < 2^\circ$

There is no radio pulsar observed in this solid angle interval which is a surprising fact since the LOSs pass through both the Local arm, the Perseus arm and the Outer arm including several SFRs. The reason may partly be the large positive offsets of the HMSFRs from the Galactic plane and also the lack of pulsar surveys for these directions.

$86^\circ < \ell < 90^\circ$; $-2^\circ < b < 2^\circ$

There are two pulsars observed in this interval; J2113+4644 ($\ell=89.003^\circ$, $b= -1.266^\circ$, $DM=141.26$ pc/cm³, $d=1.9-2.6$ kpc, $\tau = 2.25 \times 10^7$ yr) which has the Crab limits on its distance $d_{Crab} < 3.1$ kpc (S400) and $d_{Crab} < 1.7$ kpc (S1400) and J2053+4650 ($\ell=86.861^\circ$, $b=1.302^\circ$, $DM=98.0828$ pc/cm³, $\tau = 1.16 \times 10^9$ yr) (see

Table A20). Since J2113+4644 is possibly a middle aged pulsar (10^6 yr $< \tau < 10^7$ yr) with a negative latitude in this direction, its distance may be larger with respect to its DM. The kinematic distance from HI absorption measurements is $d=4\pm 1$ kpc which is in accordance with the YMW17 model but the parallax measurement (Deller et al. 2019) was used for the adopted distance ($d=2.2$ kpc) in ATNFPC. This pulsar is probably located at 2.5-3 kpc with the luminosity on the same order of magnitude as Crab's at both S400 and S1400.

4 CONCLUSIONS

Constructing distance vs DM relations is essential to determine the 3D distributions of both radio pulsars and the plasma in the Galaxy. In order to make such relations as reliable as possible, we have considered some basic criteria as presented above. Galactic distributions of the clouds and the plasma are still not well known as seen in the models on the Galactic structure. These models include significant differences with respect to each other in the locations, depths and widths of the arms even though the amount of observational data has greatly increased in recent years. This is the main factor for large uncertainties in the distances of many pulsars, especially the distant ones. Using the fact that young pulsars are located in or close to star formation regions helps to decrease these uncertainties by making comparisons. Consequently, these young pulsars are used as calibrators to improve the distance values of older ones in the same solid angle intervals.

The very large values of DM for some of the pulsars (in particular the magnetar J1745-2900) and smaller but still large DM for some other pulsars in the Galactic central directions suggest the existence of very high density plasma with possible 'gaps' for the region around the Galactic center. There is no pulsar with measured DM in the interval 600-800 pc/cm³ in the central directions. The number of radio pulsars detected in these directions being surprisingly small strengthens the probability of the presence of large density plasma in the central region.

In Taylor-Cordes (Taylor & Cordes 1993) (553 pulsars) and Cordes-Lazio (Cordes & Lazio 2002, 2003) (1143 pulsars) models, there are biases leading to underestimation of the distances for some nearby pulsars and overestimation of the distances for some distant ones. This is true especially in the Taylor-Cordes model which is based on the arm structure introduced in Georgelin and Georgelin (1976). A significant fraction (134 out of 553) of the pulsars seem to be located outside the Galaxy ($d>30$ kpc) according to the Taylor-Cordes model. Pulsars discussed in section 3.1 J1745-3040, J1740-3015 and J1752-2806 have underestimated distance values in ATNFPC (see Table 1). These distance values lead to an overestimation of the average free electron density for the region up to 0.4 kpc from the Sun in the central directions. The characteristic ages of these three pulsars are 5.46×10^5 yr, 2.06×10^4 yr, and 1.1×10^6 yr, respectively. Although they are young pulsars, with the ATNFPC adopted distances, these pulsars do not seem to be part of any Galactic arm, while with our adopted distances, J1740-3015 ($d=2.8$ kpc) is most probably located within the Scutum arm and the other two, J1752-2806 ($d=1.3$ kpc) and J1745-3040 ($d=1.7$ kpc) which have also similar RM values, are in or close to the Sagittarius arm. Our estimations on the distances of these pulsars based on comparisons with the other nearby and/or young pulsars in this group should give a more reliable average free electron density for the central directions up to about 3 kpc as well as better luminosity and space velocity values for these pulsars.

YMW17 electron distribution model (which is currently used as

Table 2. Average free electron density in the solid angle interval $358^\circ < \ell < 78^\circ$; $-2^\circ < b < 2^\circ$. n is the average free electron density in the line of sight, calculated from the inverse of the slopes of Figures 1–A19 in 1/cm³. In the solid angle interval $358^\circ < \ell < 2^\circ$; $-2^\circ < b < 2^\circ$ ⁽¹⁾ radio pulsars whose DM values are from 18 pc/cm³ to 584 pc/cm³ (see Figure 1 and Table 1) are located. In the solid angle interval $358^\circ < \ell < 2^\circ$; $-2^\circ < b < 2^\circ$ ⁽²⁾ radio pulsars whose DM values are from 835 pc/cm³ to 1133 pc/cm³ (see Figure 1 and Table 1) are located. In the solid angle interval $358^\circ < \ell < 2^\circ$; $-2^\circ < b < 2^\circ$ ⁽³⁾ radio pulsars whose DM values are 1168 pc/cm³ and 1456 pc/cm³ (see Figure 1 and Table 1) are located.

Solid Angle Interval	n 10 ⁵ /cm ³	err 10 ⁵ /cm ³
$358^\circ < \ell < 2^\circ$; $-2^\circ < b < 2^\circ$ ⁽¹⁾	7.35	± 0.27
$358^\circ < \ell < 2^\circ$; $-2^\circ < b < 2^\circ$ ⁽²⁾	9.90	± 4.80
$358^\circ < \ell < 2^\circ$; $-2^\circ < b < 2^\circ$ ⁽³⁾	5.88	± 16.90
$2^\circ < \ell < 6^\circ$; $-2^\circ < b < 2^\circ$	8.00	± 0.70
$6^\circ < \ell < 10^\circ$; $-2^\circ < b < 2^\circ$	8.20	± 0.94
$10^\circ < \ell < 14^\circ$; $-2^\circ < b < 2^\circ$	8.26	± 0.96
$14^\circ < \ell < 18^\circ$; $-2^\circ < b < 2^\circ$	8.00	± 0.58
$18^\circ < \ell < 22^\circ$; $-2^\circ < b < 2^\circ$	7.87	± 0.62
$22^\circ < \ell < 26^\circ$; $-2^\circ < b < 2^\circ$	7.52	± 0.73
$26^\circ < \ell < 30^\circ$; $-2^\circ < b < 2^\circ$	7.25	± 0.37
$30^\circ < \ell < 34^\circ$; $-2^\circ < b < 2^\circ$	9.43	± 0.36
$34^\circ < \ell < 38^\circ$; $-2^\circ < b < 2^\circ$	8.85	± 0.47
$38^\circ < \ell < 42^\circ$; $-2^\circ < b < 2^\circ$	6.33	± 0.16
$42^\circ < \ell < 46^\circ$; $-2^\circ < b < 2^\circ$	5.62	± 0.19
$46^\circ < \ell < 50^\circ$; $-2^\circ < b < 2^\circ$	4.65	± 0.26
$50^\circ < \ell < 54^\circ$; $-2^\circ < b < 2^\circ$	5.15	± 0.24
$54^\circ < \ell < 58^\circ$; $-2^\circ < b < 2^\circ$	5.13	± 0.34
$58^\circ < \ell < 62^\circ$; $-2^\circ < b < 2^\circ$	2.74	± 0.19
$62^\circ < \ell < 66^\circ$; $-2^\circ < b < 2^\circ$	3.12	± 0.16
$66^\circ < \ell < 70^\circ$; $-2^\circ < b < 2^\circ$	3.18	± 0.31
$70^\circ < \ell < 74^\circ$; $-2^\circ < b < 2^\circ$	4.98	± 2.62
$74^\circ < \ell < 78^\circ$; $-2^\circ < b < 2^\circ$	4.74	± 1.48

the default distance – DM model in ATNFPC) includes a large number of calibrator pulsars based on measurements of parallax, kinematic measurements, connections of pulsars to other sources and clusters. ATNFPC adopted distances are significantly different for some pulsars as compared to YMW17, especially the ones based on kinematic measurements. As the minimum and maximum limits on pulsar distances from kinematic measurements differ significantly in many cases, we do not use kinematic distances for the calibration of distance – DM relations in our model.

Although, there are more than 8000 plasma regions observed up to date (see e.g. WISE catalogue 2021 Anderson et al. 2014), distribution of the HII regions in the Galaxy is highly uncertain and the density distributions within HII regions are unknown. Because of the lack of information on the contribution of each HII to DM and the large uncertainty in their distances, it is possible only to determine the average free electron density in different directions (see Table 2). In order to get the average densities of plasma, all the available data directly or indirectly related to the locations of radio pulsars, HII regions, SNRs and molecular clouds are taken into consideration in this work. Distance – DM relations for pulsars in solid angle intervals relate the distribution of pulsars to the distribution of plasma in each interval. Making comparisons between pulsars in each solid angle

interval improves such relations. As the number of known radio pulsars and their observational data increased significantly in the last decade, it is now possible to get more reliable distance – DM relations in small solid angle intervals following the works by Guseinov et al. (2002, 2007).

ACKNOWLEDGEMENTS

This work was supported by TUBITAK through project no: 115F028.

DATA AVAILABILITY

The data underlying this article are available in the article.

REFERENCES

- Abdo A. A., et al., 2013, *ApJS*, **208**, 17
- Allakhverdiev A. O., Guseinov O. H., Tagieva S. O., Yusifov I. M., 1997, *Astronomy Reports*, **41**, 257
- Anderson L. D., Bania T. M., Balsler D. S., Cunningham V., Wenger T. V., Johnstone B. M., Armentrout W. P., 2014, *ApJS*, **212**, 1
- Ankay A., Yazgan E., Kutukcu P., 2016, *SerAJ*, **193**, 1
- Archibald R. F., et al., 2016, *ApJ*, **819**, L16
- Arumugasamy P., Pavlov G. G., Kargaltsev O., 2014, *ApJ*, **790**, 103
- Arzoumanian Z., Gotthelf E. V., Ransom S. M., Safi-Harb S., Kothes R., Landecker T. L., 2011, *ApJ*, **739**, 39
- Backer D. C., Kulkarni S. R., Heiles C., Davis M. M., Goss W. M., 1982, *Nature*, **300**, 615
- Bagchi M., 2013, *IJMPD*, **22**, 1330021
- Bartkiewicz A., Brunthaler A., Szymczak M., van Langevelde H. J., Reid M. J., 2008, *ApJ*, **490**, 787
- Baumgardt H., Hilker M., Sollima A., Bellini A., 2019, *MNRAS*, **482**, 5138
- Bisnovatyi-Kogan G. S., Komberg B. V., 1974, *SvA*, **18**, 217
- Bisnovatyi-Kogan G. S., Komberg B. V., 1976, *PAZh*, **2**, 338
- Brunthaler A., Reid M. J., Menten K. M., Zheng X. W., Moscadelli L., Xu Y., 2009, *ApJ*, **693**, 424
- Camilo F., Manchester R. N., Gaensler B. M., Lorimer D. R., 2002, *ApJ*, **579**, L25
- Caswell J. L., Kesteven M. J., Komesaroff M. M., Haynes R. F., Milne D. K., Stewart R. T., Wilson S. G., 1987, *MNRAS*, **225**, 329
- Choi Y. K., Hachisuka K., Reid M. J., Xu Y., Brunthaler A., Menten K. M., Dame T. M., 2014, *ApJ*, **790**, 99
- Cohn H. N., Lugger P. M., Grindlay J. E., Edmonds P. D., 2002, *ApJ*, **571**, 818
- Cordes J. M., Lazio T. J. W., 2002, arXiv e-prints, [pp astro-ph/0207156](#)
- Cordes J. M., Lazio T. J. W., 2003, arXiv e-prints, [pp astro-ph/0301598](#)
- Deller A. T., et al., 2019, *ApJ*, **875**, 100
- Ding H., et al., 2020, *MNRAS*, **498**, 3736
- Espinoza C. M., Lyne A. G., Kramer M., Manchester R. N., Kaspi V. M., 2011, *ApJ*, **741**, L13
- Faucher-Giguère C.-A., Kaspi V. M., 2006, *ApJ*, **643**, 332
- Ferraro F. R., et al., 2009, *Nature*, **462**, 1028
- Frail D., Kulkarni S., 1991, *Nature*, **352**, 785
- Frail D. A., Kassim N. E., Weiler K. W., 1994, *AJ*, **107**, 1120
- García P., Bronfman L., Nyman L.-Å., Dame T. M., Luna A., 2014, *ApJS*, **212**, 2
- Georgelin Y. M., Georgelin Y. P., 1976, *A&A*, **49**, 57
- Green D. A., 2019, *JApA*, **40**, 36
- Guseinov O. H., Yazgan E., Tagieva S., Yoldas A. K., 2002, arXiv preprint [astro-ph/0207306](#)
- Guseinov O. H., Yazgan E., Tagieva S. O., Ozkan S., 2003a, *Rev. Mex. Astron. Astrofis.*, **39**, 267
- Guseinov O. H., Ankay A., Tagieva S. O., 2003b, *SerAJ*, **167**, 93
- Guseinov O. H., Ankay A., Tagieva S. O., 2004, *IJMPD*, **13**, 1805
- Guseinov O. H., Yazgan E., Ankay A., 2007, *Neutron Stars, Supernovae and Supernova Remnants*. Nova Science Publishers, New York
- Hachisuka K., Choi Y. K., Reid M. J., Brunthaler A., Menten K. M., Sanna A., Dame T. M., 2015, *ApJ*, **800**, 2
- Hansen B. M. S., Phinney E. S., 1997, *MNRAS*, **291**, 569
- Harris W. E., 1996, *AJ*, **112**, 1487
- Hessels J., Roberts M., Ransom S., Kaspi V., Romani R., Ng C.-Y., Freire P., Gaensler B., 2004, *ApJ*, **612**, 389
- Hou L. G., Han J. L., 2014, *A&A*, **569**, A125
- Hou L. G., Han J. L., Shi W. B., 2009, *A&A*, **499**, 473
- Immer K., Reid M. J., Menten K. M., Brunthaler A., Dame T. M., 2013, *A&A*, **553**, A117
- Jiang L., Zhang C.-M., Tanni A., Zhao H.-H., 2013, *IJMPS*, **23**, 95
- Katsuda S., et al., 2018, *ApJ*, **856**, 18
- Kirichenko A., et al., 2015, *ApJ*, **802**, 17
- Kong A. K. H., Hui C. Y., Cheng K. S., 2010, *ApJ*, **712**, L36
- Kurayama T., Nakagawa A., Sawada-Satoh S., Sato K., Honma M., Sunada K., Hirota T., Imai H., 2011, *PASJ*, **63**, 513
- Lee J.-W., Koo B.-C., Lee J.-E., 2012, *JKAS*, **45**, 117
- Lee Y.-H., Koo B.-C., Lee J.-J., Burton M. G., Ryder S., 2019, *AJ*, **157**, 123
- Lipunov V. M., 1992, *Astrophysics of Neutron Stars*. Springer-Verlag Berlin Heidelberg
- Lyne A., Graham-Smith F., 2012, *Pulsar astronomy*. No. 48, Cambridge University Press
- Lyne A. G., Pritchard R. S., Graham-Smith F., Camilo F., 1996, *Nature*, **381**, 497
- Lyne A. G., Stappers B. W., Keith M. J., Ray P. S., Kerr M., Camilo F., Johnson T. J., 2015, *MNRAS*, **451**, 581
- Manchester R. N., Taylor J. H., 1977, *Pulsars*
- Manchester R. N., Hobbs G. B., Teoh A., Hobbs M., 2005, *AJ*, **129**, 1993
- Matthews A. M., et al., 2016, *ApJ*, **818**, 92
- Ortolani S., Barbuy B., Bica E., 1996, *A&A*, **308**, 733
- Ortolani S., Barbuy B., Bica E., Renzini A., Zoccali M., Rich R. M., Cassisi S., 2001, *A&A*, **376**, 878
- Ortolani S., Barbuy B., Bica E., Zoccali M., Renzini A., 2007, *A&A*, **470**, 1043
- Petroff E., Keith M. J., Johnston S., van Straten W., Shannon R. M., 2013, *MNRAS*, **435**, 1610
- Ponti G., et al., 2015, *MNRAS*, **453**, 172
- Radhakrishnan V., Goss W. M., Murray J. D., Brooks J. W., 1972, *ApJS*, **24**, 49
- Ranasinghe S., Leahy D. A., 2018, *AJ*, **155**, 204
- Reardon D. J., et al., 2016a, *MNRAS*, **455**, 1751
- Reardon D. J., et al., 2016b, *MNRAS*, **455**, 1751
- Reid M. J., Menten K. M., Zheng X. W., Brunthaler A., Xu Y., 2009, *ApJ*, **705**, 1548
- Reid M. J., et al., 2014, *ApJ*, **783**, 130
- Reid M. J., et al., 2019, *ApJ*, **885**, 131
- Rygl K. L. J., et al., 2012, *A&A*, **539**, A79
- Sanna A., Reid M. J., L. M., Dame T. M., Menten K. M., Brunthaler A., Zheng X. W., Xu Y., 2009, *ApJ*, **706**, 464
- Sanna A., Reid M. J., Dame T. M., Menten K. M., Brunthaler A., Moscadelli L., Zheng X. W., Xu Y., 2012, *ApJ*, **745**, 82
- Sanna A., et al., 2014, *ApJ*, **781**, 108
- Sato M., Hirota T., Reid M. J., Honma M., Kobayashi H., Iwadate K., Miyajima T., Shibata K. M., 2010, *PASJ*, **62**, 287
- Sato M., et al., 2014, *ApJ*, **793**, 72
- Schnitzeler D. H. F. M., Eatough R. P., Ferrière K., Kramer M., Lee K. J., Noutsos A., Shannon R. M., 2016, *MNRAS*, **459**, 3005
- Shan S. S., Zhu H., Tian W. W., Zhang M. F., Zhang H. Y., Wu D., Yang A. Y., 2018, *ApJS*, **238**, 35
- Taylor J. H., Cordes J. M., 1993, *ApJ*, **411**, 674
- Thorstett S. E., Brisken W. F., Goss W. M., 2002, *ApJ*, **573**, L111
- Tian W. W., Leahy D. A., 2008, *MNRAS*, **391**, L54
- Uchida K., Morris M., Yusef-Zadeh F., 1992, *AJ*, **104**, 1533
- Valenti E., Ferraro F. R., Origlia L., 2007, *AJ*, **133**, 1287
- Vallée J. P., 2014a, *AJ*, **148**, 5
- Vallée J. P., 2014b, *ApJS*, **215**, 1

Vallée J. P., 2015, *MNRAS*, **450**, 4277
 Velázquez P. F., Dubner G. M., Goss W. M., Green A. J., 2002, *AJ*, **124**, 2145
 Verbunt F., Igoshev A., Cator E., 2017, *A&A*, **608**, A57
 Wu Y. W., et al., 2014, *A&A*, **566**, A17
 Wu Y. W., et al., 2019, *ApJ*, **874**, 94
 Xu Y., Reid M. J., Menten K. M., Brunthaler A., Zheng X. W., Moscadelli L., 2009, *ApJ*, **693**, 413
 Xu Y., Moscadelli L., Reid M. J., Menten K. M., Zhang B., Zheng X. W., Brunthaler A., 2011, *ApJ*, **733**, 25
 Xu Y., et al., 2013, *ApJ*, **769**, 15
 Yao J. M., Manchester R. N., Wang N., 2017, *ApJ*, **835**, 29
 Yazgan E., Guseinov O. H., Tagieva S., 2007, in Lowry J., ed., *Trends in Pulsar Research*. Nova Science Publishers, pp 1–24
 Zhang B., Zheng X. W., Reid M. J., Menten K. M., Xu Y., Moscadelli L., Brunthaler A., 2009, *ApJ*, **693**, 419
 Zhang B., Reid M. J., Menten K. M., Zheng X. W., Brunthaler A., 2012, *A&A*, **544**, A42
 Zhang B., Reid M., Menten K., Zheng X., Brunthaler A., Dame T., Xu Y., 2013, *ApJ*, **775**, 79
 Zhang B., et al., 2014, *ApJ*, **781**, 89

APPENDIX A: FIGURES AND TABLES

Figures and tables for distance-DM relations in the solid angle interval $2^\circ < \ell < 90^\circ$; $-2^\circ < b < 2^\circ$ are given in this section.

Table A1. Radio pulsars in the solid angle interval $2^\circ < \ell < 6^\circ$; $-2^\circ < b < 2^\circ$ with measured DM. See Table 1 for column descriptions.

PSR	Data from ATNFPC						Adopted and Calculated Data in this Study						
	ℓ degree	b degree	DM pc/cm ³	err pc/cm ³	RM rad/m ²	err rad/m ²	τ Myr	RM/DM kpc	d kpc	err kpc	d_{Crab} kpc	z	
J1755-2725	2.432	-1.135	115	± 5	-	-	302	-	2.2	+0.4, -0.3	11	-44	
J1750-2536	3.413	0.778	1784	± 0.01	-	-	-	3	+0.4, -0.3	12	41		
J1757-2421	5.281	0.054	179.454	± 0.011	16	± 5.0	0.285	0.09	3	± 0.3	10.5 ²	2.8	3
J1748-2444	3.955	1.564	207.33	± 0.09	-	-	63	-	3.4	± 1.3	13	93	
J1748-2440	4.263	-0.807	218.2	± 1.3	-207	± 9.3	21.5	-0.95	3.4	± 0.4	9	-48	
J1748-2446A	3.836	1.696	242.15	± 0.04	-	-	-	-	5	$\pm 2.0, -1$	10	148	
J1755-2521	4.255	-0.15	252	± 4	34.6	± 6.8	0.207	0.14	3.5	± 0.4	9	-9	
J1805-2447	5.807	-1.725	269	± 3	-	-	1800	-	4.2	± 1.5	14	-126	
J1801-2451	5.254	-0.882	291.55	± 0.05	605.7	± 0.5	0.0155	2.08	4.5	± 0.5	16.8 ³ , 6.2	-69	
J1758-2630	3.555	-1.225	328	± 3	-	-	3.69	-	5.5	± 1.7	12	-118	
J1750-2444	4.136	1.255	331	± 4	-	-	54	-	5	± 1.6	14	110	
J1757-27	2.4	-1.721	334	± 0.1	-	-	1330	-	5.1	± 1.6	28	-153	
J1749-2347	4.828	1.967	344	± 4	-	-	5.72	-	5.5	± 1.7	21	189	
J1756-2435	5.027	0.044	367.1	± 0.4	-130	± 7.0	3.73	-0.35	5	± 0.5	16.2 ¹ , 5.3	4	
J1755-26	3.618	-0.333	405	± 4	-	-	0.556	-	5.5	± 0.6	20	-32	
J1749-2629	2.505	0.973	409	± 11	916	± 17.0	12.3	2.24	5.7	± 0.6	9	59	
J1759-2549	4.261	-1.082	431	± 5	93	± 14	0.152	0.22	6.5	± 2.0	10	-123	
J1750-2438	4.291	1.185	476	± 5	564	± 13.0	1.05	1.18	7.4	± 2.2	11	153	
J1752-2410	4.93	1.039	508.3	± 0.9	-153	± 24.0	4.9	-0.3	7.5	± 2.2	11	136	
J1756-2919	3.574	-0.891	534	± 2	-	-	3.27	-	7.7	± 1.2	24	-120	
J1751-2516	3.852	0.692	556	± 3	-	-	2.37	-	8	± 2.4	16	97	
J1747-2647	2.054	0.758	570	± 9	-	-	0.599	-	8.2	± 2.2	6	108	
J1755-2534	4.047	-0.229	590	± 3	-	-	0.33	-	8.4	± 2.4	18	-34	
J1755-2501	4.274	0.512	672	± 3	21	± 17	0.593	0.03	9	± 2.7	-	80	
J1756-25	4.241	-0.342	706	± 8	-	-	-	-	10	± 2.6	17	-60	
J1802-2426	5.731	-0.886	711	± 6	74	13	1.05	0.1	10	± 3.0	10	-155	
J1754-2422	4.947	0.618	738	± 6	-	-	39.9	-	10.4	± 2.7	-	112	
J1755-2550	3.799	-0.323	750.9	± 0.4	-	-	2.05	-	10.6	± 2.7	17	-60	
J1759-24	5.789	-0.156	772	± 14	-	-	-	-	10.8	± 2.8	11	-29	
J1755-25311	4.183	-0.016	835	± 5	-	-	0.51	-	11.7	± 3.0	18	-3	

Table A2. Radio pulsars in the solid angle interval $6^\circ < \ell < 10^\circ$; $-2^\circ < b < 2^\circ$ with measured DM. See Table 1 for column descriptions.

PSR	Data from ATNFPC						Adopted and Calculated Data in this Study					
	ℓ degree	b degree	DM pc/cm ³	err pc/cm ³	RM rad/m ²	err rad/m ²	τ Myr	RM/DM kpc	d kpc	err kpc	d_{Crab} kpc	z
J1756-2251	6.499	0.948	121.196	± 0.005	10	± 11.0	443	0.08	2.1	± 1.0	10	35
J1802-2124	8.382	0.611	149.6258	± 0.0006	286	± 14.0	2760	1.91	2.5	± 1.0	9	27
J1753-2240	6.299	1.663	158.6	± 0.4	-	-	1550	-	2.6	± 1.0	19	75
J1759-2205	7.472	0.81	177.157	± 0.005	6	± 7.0	0.673	0.03	2.9	± 0.3	10.5 ¹ , 6.6	41
J1803-2137	8.395	0.146	233.99	± 0.05	-36.1	± 0.2	0.0158	-0.15	3.3	± 1.0	9.8 ¹ , 2.4	8
J1759-1956	9.366	1.845	236.4	± 1.9	-	-	2.43	-	3.5	± 1.1	12	113
J1757-2223	7.029	0.97	239.3	± 0.4	-145.2	± 4.7	3.75	-0.61	3.5	± 1.1	8	59
J1800-2343	6.132	-0.118	280	± 40	-	-	-	-	4	± 1.2	23 ¹	-8
J1759-1940	9.634	1.901	302.7	± 1	775	± 16.0	43.2	2.56	4.5	± 1.4	8	149
J1756-2225	6.835	1.237	329	± 1	-	-	0.122	-	4.6	± 1.4	15	99
J1809-2109	9.415	-0.72	381.91	± 0.05	256	± 24.0	2.91	0.67	5.5	± 1.7	8	-69
J1801-2154	7.838	0.554	386	± 1	160	± 40.0	0.371	0.41	5.4	± 1.5	16	52
J1804-2228	7.722	-0.397	424	± 7	-	-	63.1	-	5.5	± 1.7	17	-38
J1812-20	9.954	-1.321	457	± 19	-	-	126	-	6.4	± 2.0	-	-146
J1813-2113	9.853	-1.656	462.3	± 1.5	417.9	± 8.2	3.25	0.9	6.5	± 2.0	10	-188
J1812-1102	9.859	1.904	547.2	± 1	322.6	± 4.2	0.811	0.59	7.5	± 3.3	6	-171
J1808-2057	8.446	-0.4	606.8	± 0.9	93	± 11.0	0.852	0.15	8	± 2.4	5	-56
J1800-2114	9.306	1.073	641	± 18	-	-	51.8	-	8.5	± 2.0	14	159
J1758-2206	7.378	0.933	678	± 4	-	-	7.13	-	9	± 2.7	12	147
J1805-2037	9.449	0.307	708.1	± 1.6	-	-	3.23	-	9	± 2.7	13	48
J1806-2125	8.811	-0.28	747	± 1	796	± 15.0	0.0647	1.07	10	± 3.0	8	-49
J1801-2115	8.446	0.794	778.8	± 0.1	-	-	446	-	10	$\pm 2.5, -2.2$	17	139
J1759-1940	9.591	1.904	805	± 1.5	743	± 11.0	2.35	0.91	11	± 3.0	11	53
J1759-2302	6.702	0.257	889	± 1	1575	± 13.0	1.2	1.77	12	± 3.6	7	54
J1805-2032	9.53	0.313	932.3	± 2	-	-	0.766	-	12	± 3.6	9	66
J1801-2304	6.837	-0.066	1073.9	± 0.6	-1156	± 19.0	0.0583	-1.08	13.5	± 4.1	3	-16

Table A3. Radio pulsars in the solid angle interval $10^\circ < \ell < 14^\circ$; $-2^\circ < b < 2^\circ$ with measured DM. See Table 1 for column descriptions.

PSR	Data from ATNFPC						Adopted and Calculated Data in this Study					
	ℓ degree	b degree	DM pc/cm ³	err pc/cm ³	RM rad/m ²	err rad/m ²	τ Myr	RM/DM kpc	d kpc	err kpc	d_{Crab} kpc	z
J1809-1943	10.727	-0.158	178	± 5	76	± 1.0	0.031	0.43	3	± 0.3	9	-8
J1809-1917	11.094	0.068	197.1	± 0.4	41	± 17.0	0.0514	0.21	3.3	± 0.4	4	5
J1810-2005	10.545	-0.563	241	± 0.3	-15	± 14.0	3530	-0.06	4	± 0.5	6	-39
J1812-1718	13.109	0.538	255.1	± 1.8	70.6	± 8.9	1	0.28	4.2	± 0.5	7	39
J1801-1909	10.295	1.781	264	± 9	-	-	25	-	5	± 1.0	11	155
J1803-1857	10.73	1.428	292	± 1.1	788.6	± 9.2	2.99	2.01	5.9	± 2.0	12	147
J1819-1717	13.951	-1.048	405	± 2	-	-	1.8	-	5.8	± 1.7	15	-107
J1820-1818	13.202	-1.472	436	± 1.2	-70	± 12.0	52.5	-0.16	7.5	± 2.3	6	-225
J1803-1920	10.334	1.338	436.1	± 1.7	-	-	21.3	-	8.2	± 2.1	14	191
J1810-1820	12.064	0.289	452.2	± 2.5	110.3	± 8.1	46.6	0.24	5.6	± 1.7	9	28
J1811-1736	12.821	0.435	476	± 5	-	-	1830	-	5.9	± 1.8	7	45
J1801-1855	10.447	1.978	484	± 14	424	± 15.0	222	0.88	9.2	± 2.4	11	318
J1812-1733	12.904	0.387	518	± 4	342.6	± 2.8	8.68	0.66	6.3	± 1.9	3	43
J1817-1938	11.623	-1.617	519.6	± 0.01	-	-	90.1	-	8.9	± 2.7	24	-251
J1816-1729	13.433	-0.424	525.5	± 0.7	82.9	± 4.1	1.71	0.16	6.5	± 2.0	7	-48
J1808-1726	12.599	1.188	536	± 7	-	-	329	-	7.6	± 2.3	12	158
J1811-1717	13.041	0.686	545.5	± 0.01	-	-	51.7	-	7.6	± 2.3	17	91
J1815-1910	11.81	-0.963	547.8	± 0.4	-	-	0.546	-	7.8	± 2.3	13	-131
J1809-1850	11.473	0.316	598	± 13	-	-	1.68	-	7.5	± 2.5	17	41
J1811-1709	13.051	1.956	670	± 20	-	-	55.2	-	9.7	± 3.0	11	162
J1806-1920	10.641	0.802	683	± 7	1069	± 14.0	819	1.57	9.5	± 3.0	6	133
J1815-1738	13.179	-0.272	724.6	± 0.2	175	± 20.0	0.0404	0.24	9.2	± 2.8	12	-44
J1811-1835	11.909	0.049	761	± 11	-345	± 18.0	1.4	-0.45	9.5	± 2.9	12	8
J1814-1649	13.82	0.245	782	± 6	-857	± 12.0	2.4	-1.1				

Table A5. Radio pulsars in the solid angle interval $18^\circ < \ell < 22^\circ$; $-2^\circ < b < 2^\circ$ with measured DM. See Table 1 for column descriptions.

PSR	Data from ATNFPC							Adopted and Calculated Data in this Study						
	ℓ degree	b degree	DM pc/cm ³	err pc/cm ³	RM rad/m ²	err rad/m ²	τ Myr	RM/DM kpc	d kpc	err kpc	d_{Crab} kpc	z	pc	
J1825-0935	21.449	1.324	19.3833	± 0.0009	65.2	± 0.2	0.233	3.36	1	± 0.2	7.8 ¹ , 2.3	23		
J1835-1020	21.98	-1.302	113.7	± 0.9	142.8	± 3.2	0.81	1.26	2.6	± 0.8	5	-59		
J1825-1108	20.047	0.641	121	± 19	-	-	16.1	-	2	± 0.6	21	22		
J1835-1106	21.222	-1.513	132.679	± 0.003	42.9	± 2.1	0.128	0.32	2.8	± 0.4	8.6 ¹ , 4.7	-74		
J1830-1059	20.802	-0.478	159.7	± 0.01	47	± 5.0	0.107	0.29	2.9	± 0.5	32.4 ¹ , 6.1	-54		
J1833-1034	21.511	-0.885	169.5	± 0.1	-	-	0.00485	-	3.5	± 1.0	-0.5	28	-74	
J1830-10	21.036	-0.169	203	± 2	-	-	-	-	3	± 0.9	24	-9		
J1826-1310	18.001	-0.691	251	± 1	10	± 5.0	0.0214	0.04	3.5	± 0.5	3	-42		
J1831-0952	21.897	-0.128	247	± 5	0.2	± 8.0	0.128	0.001	3.5	± 0.5	13	-8		
J1828-1057	20.587	0.024	249	± 2	-	-	0.189	-	3.5	± 0.5	13	1		
J1830-1135	20.193	-0.59	257	± 6	249.4	± 7.8	2.06	0.97	4.4	± 1.3	7	-45		
J1827-0934	21.724	0.841	259.2	± 0.5	-386	± 24.0	1.12	-1.49	4.5	± 1.4	14	66		
J1828-1007	21.324	0.424	302.6	± 1.2	-	-	3.96	-	4.5	± 1.4	16	33		
J1819-1114	19.291	1.857	310	± 5	-	-	8.23	-	5.4	± 1.6	7	175		
J1826-1131	19.48	0.203	320.58	± 0.06	229	± 23.0	6.75	0.71	4.8	± 1.4	21 ¹ , 8.9	25		
J1836-11	21.118	-1.768	326	± 8	-	-	5.7	-	5.7	± 1.7	22	-176		
J1831-1329	18.716	-1.884	338	± 5	374	± 4.8	11.5	1.11	5.9	± 1.8	11	-194		
J1831-1223	19.618	-1.217	342	± 5	-41.3	± 4.3	8.27	-0.12	5.5	± 1.7	7	-117		
J1834-1202	20.287	-1.743	342.4	± 1.3	-253	± 7.7	1430	-0.74	6	± 1.8	9	-182		
J1823-1115	19.767	0.946	428.59	± 0.09	-354	± 10.0	3.22	-0.83	6.1	± 1.8	14.1 ¹ , 4.2	101		
J1827-0958	21.286	0.798	430	± 4	-42	± 19.0	3.88	-0.1	7.6	± 2.3	5	106		
J1824-1159	19.253	0.324	463.4	± 2.4	407	± 15.0	1.07	0.88	6.1	± 1.8	9	34		
J1832-1021	21.587	-0.597	475.7	± 0.3	103.8	± 5.6	1.25	0.22	7.9	± 2.4	25.4 ¹ , 5.4	-82		
J1828-1336	18.254	-1.243	494.7	± 1.8	-	-	13.7	-	7.2	± 2.2	15	-156		
J1830-1313	18.824	-1.49	537	± 3	-	-	6.91	-	9	± 2.7	15	-234		
J1833-1055	21.231	-1.14	543	± 4	42	± 9.5	19.1	0.08	8.4	± 2.5	11	-167		
J1819-1131	19.101	1.619	578	± 13	-	-	28.9	-	10	± 3.0	19	283		
J1824-1118	19.809	0.741	603	± 2	213	± 17.0	1.94	0.35	8.1	± 2.4	7	105		
J1828-1101	20.495	0.043	605	± 0.1	59.4	± 2.5	0.0772	0.1	7.3	± 2.2	5	5		
J1823-1126	19.568	0.935	607	± 3	-	-	8.01	-	8.6	± 2.6	10	140		
J1829-1011	21.239	0.262	610	± 0.1	-	-	-	-	7.8	± 2.3	15	36		
J1822-1252	18.218	0.394	925	± 25	-	-	0.387	-	12.3	± 3.7	15	85		

Table A6. Radio pulsars in the solid angle interval $22^\circ < \ell < 26^\circ$; $-2^\circ < b < 2^\circ$ with measured DM. See Table 1 for column descriptions.

PSR	Data from ATNFPC							Adopted and Calculated Data in this Study						
	ℓ degree	b degree	DM pc/cm ³	err pc/cm ³	RM rad/m ²	err rad/m ²	τ Myr	RM/DM kpc	d kpc	err kpc	d_{Crab} kpc	z	pc	
J1832-0836	23.109	0.257	28.19422	± 0.00009	25	± 17.0	5210	0.89	1	± 0.5	7	-4		
J1830-0627	25.807	-0.266	88.5	± 0.7	-	-	58.3	-	2.1	± 0.6	14	-10		
J1842-0800	24.829	-1.766	188.6	± 0.01	-	-	103	-	3.5	± 1.1	24	-108		
J1835-0946	22.451	-0.999	193.3	± 0.5	-	-	139	-	3.1	± 0.9	18	-54		
J1843-0806	24.806	-1.934	215.8	± 0.9	167	± 15.0	0.49	0.77	4	± 1.2	12	-135		
J1843-0702	25.741	-1.426	228.4	± 0.2	-	-	1.42	-	4	± 1.2	14	-100		
J1840-0815	24.314	-1.283	233.2	± 1.2	178.7	± 7.7	7.16	0.77	4	± 1.2	5	-90		
J1831-0823	23.211	0.548	245.9	± 1.7	54.3	± 3.7	31.4	0.22	4.3	± 1.3	7	41		
J1840-0840	24.01	-1.616	272	± 19	564.5	± 5.1	3.55	2.08	4.7	± 1.4	6	-133		
J1835-0944	22.487	-0.989	276.2	± 0.1	236.2	± 9.0	0.525	0.86	4.5	± 1.4	10	-78		
J1834-0731	24.288	0.366	294	± 0.9	92.6	± 8.5	0.14	0.31	4.7	± 1.4	7	30		
J1832-0827	23.272	0.298	300.869	± 0.01	39	± 7.0	0.161	0.13	4.8	± 1.4	15.3 ¹ , 3.7	25		
J1837-0653	25.191	0.002	316.1	± 0.4	-268.4	± 4.1	39.1	-0.85	5	± 1.5	4	0		
J1829-0734	23.647	1.478	316.8	± 1.8	263	± 17.0	1.05	0.83	5.5	± 1.7	11	142		
J1836-1008	22.263	-1.415	316.98	± 0.03	826.6	± 4.5	0.756	2.61	5.5	± 1.7	6.4 ¹ , 3.4	-136		
J1843-0744	25.092	-1.68	321	± 5	-	-	0.566	-	5.8	± 1.7	18	-170		
J1839-0905	23.533	-1.591	344.5	± 0.3	-	-	0.255	-	6	± 1.8	16	-137		
J1840-0809	24.441	-1.308	349.8	± 0.8	262.6	± 2.5	6.44	0.75	6	± 1.8	5	-167		
J1833-0559	25.514	1.321	353	± 6	-	-	0.62	-	5.8	± 1.7	10	134		
J1827-0750	23.176	1.803	381	± 9	401.9	± 2.7	2.77	-1.05	7	± 2.1	4	220		
J1833-0827	23.386	0.063	410.95	± 0.1	-470	± 7.0	0.147	-1.14	5.7	± 1.7	3	6		
J1838-0624	25.792	-1.14	424	± 9	-	-	190	-	5.5	± 1.7	19	-113		
J1834-0602	25.64	0.965	445	± 4	380	± 11.0	4.23	0.85	6.6	± 2.0	8	-111		
J1835-0928	22.684	-0.774	450	± 0.1	-	-	10.2	-	6.5	± 2.0	9	-88		
J1837-0604	25.96	0.265	459.3	± 0.3	320.8	± 4.2	0.0338	0.7	6.2	± 1.9	9	29		
J1835-0556	25.623	1.232	461	± 13	-	-	18.8	-	7	± 2.1	17	151		
J1835-0643	25.093	0.552	467.9	± 0.4	44	± 15.0	0.12	0.09	6.5	± 2.0	5	63		
J1833-0924	22.767	-0.804	471	± 7	-	-	0.636	-	6.8	± 2.0	10	-95		
J1840-0643	25.662	-0.567	494	± 0.1	-	-	5910	-	6.6	± 2.0	7	-65		
J1839-0643	25.547	-0.35	497.9	± 1.6	-297.7	± 18.0	1.96	-5.98	6.5	± 2.0	6	-179		
J1835-0942	22.739	-0.744	500	± 0.1	-	-	315	-	7.2	± 2.2	-	-93		
J1837-0822	23.918	-0.772	506	± 0.1	-	-	144	-	7.3	± 2.2	17	-98		
J1834-09	22.789	-0.505	529	± 7	-	-	-	-	7.3	± 2.2	18	-64		
J1834-0742	24.151	0.223	552	± 18	-	-	0.385	-	7.7	± 2.3	13	30		
J1835-0644	24.806	1.07	578	± 7	226	± 11.0	0.318	0.39	9	± 2.7	9	168		
J1840-0753	24.698	-1.242	691	± 7	-	-	69.4	-	11	± 3.3	12	-238		
J1834-0633	25.173	0.763	707	± 9	-	-	8.32	-	11	± 3.3	14	146		
J1840-0626	25.933	-0.461	748	± 8	-	-	1.3	-	11	± 3.3	19	-89		
J1835-0600	25.758	0.829	780	± 20	-	-	4.18	-	12	± 3.5	5	-174		
J1835-0847	23.331	-0.548	850	± 0.1	-	-	27.7	-	13	± 3.5	12	-124		
J1834-0812	23.709	0.081	1020	± 50	-	-	0.781	-	14	± 4.0	10	-224		

Table A7. Radio pulsars in the solid angle interval $26^\circ < \ell < 30^\circ$; $-2^\circ < b < 2^\circ$ with measured DM. See Table 1 for column descriptions.

PSR	Data from ATNFPC							Adopted and Calculated Data in this Study						
	ℓ degree	b degree	DM pc/cm ³	err pc/cm ³	RM rad/m ²	err rad/m ²	τ Myr	RM/DM kpc	d kpc	err kpc	d_{Crab} kpc	z	pc	
J1841-04	27.49	0.09	29	± 3	-	-	-	-	0.7	± 0.2	-	1		
J1840-0317	29.834	-1.173	42.9	± 2.8	-31.9	± 3.8	0.481	-0.74	1.5	± 0.5	9	-31		
J1834-0426	27.042	1.749	79.308	± 0.008	100	± 5.0	63.9	1.26	3.3	± 0.5	5.3 ¹ , 3.3	70		
J1844-0433	28.096	-0.548	123.158	± 0.02	7	± 13.0	40.1	0.06	2.4	± 1.0	-0.5	16.5 ¹ , 7.1	-23	
J1847-0402	28.876	-0.939	141.979	± 0.005	117	± 8.0	0.183	0.82	3.5	± 0.5	-0.3	5.4 ¹ , 3.4	-57	
J1842-0415	28.086	0.111	188	± 4	-90	± 15.0	0.38	-0.48	3.6	± 0.4	-0.2	13	7	
J1847-0427	28.487	-1.12	188.3	± 0.01	-	-	696	-	4	± 0.5	-	-78		
J1841-0345	28.424	0.437	194.32	± 0.06	450.5	± 2.6	0.0559	2.32	3.8	± 0.4	-0.2	7	29	
J1839-0332	28.462	0.934	195.1	± 0.01	-	-	8.91	-	4	± 0.5	-			

Table A9. Radio pulsars in the solid angle interval $34^\circ < \ell < 38^\circ$; $-2^\circ < b < 2^\circ$ with measured DM. See Table 1 for column descriptions.

PSR	Data from ATNFPC							Adopted and Calculated Data in this Study										
	ℓ degree	b degree	DM pc/cm ³	err pc/cm ³	RM rad/m ²	err rad/m ²	τ Myr	RMDM kpc	err kpc	d_{Crab} kpc	z	RMDM kpc	err kpc	d_{Crab} kpc	z			
J1857+0057	34.417	-0.805	82.39		104	±19.0	104	1.26	2.4	+0.5, -0.3	21.7, 7.8	-	1.2	+0.4, -0.2	70.7, 13.8	-0		
J1856+0113	34.56	-0.497	96.74		±0.12	±30.0	0.0203	-1.45	2.8	+0.3	25.4 ¹ , 17.2	-	2.4	+0.3	34.2, 8	-53		
J1901+0156	35.818	-1.367	105.394		±0.007	-122	±9.0	1.94	-1.16	3.2	+0.5, -0.3	12.7, 1.2	-76	-	-	-		
J1850+0124	34.025	0.959	118.89		±0.05	-	-	5.180	3	+0.5	17	50	-	3	+0.5	12	-36	
J1853+0056	34.017	-0.036	180.9		±1.2	-	-	0.204	3.8	+0.3	16	-2	-	3.61	2.9	+0.3, -0.5	44.7, 10.1	10
J1901+0254	36.643	-0.855	185		±5	-121.7	±8.5	45.2	-0.66	4	+0.5, -0.3	10	-60	-	-	-	-	-
J1854+0306	35.992	0.834	192.4		±5.2	-	-	0.498	4.2	+0.5, -0.3	13	61	-	-	-	-	-	-
J1900+0227	36.17	-0.925	201.1		±1.7	-52	±30.0	1.04	-0.26	4.3	+0.5, -0.3	13	-69	-	-	-	-	-
J1849+0127	34.034	1.043	207.3		±2.6	-165	±12.0	3.07	-0.8	4.6	+0.8, -0.5	11	84	-	-	-	-	-
J1903+0135	35.727	-1.955	245.167		±0.006	72.3	±1.0	2.87	0.29	5.4	+1.0, -0.5	6.2 ¹ , 3.2	-184	-	-	-	-	-
J1857+0143	35.168	-0.571	249		±3	41.9	±4.3	0.071	1.7	4.7	+0.5	9	-47	-	-	-	-	-
J1900+0308	36.798	-0.658	249.898		±0.011	-	-	13200	-	4.8	+0.5	24	-55	-	-	-	-	-
J1901+0300	36.811	-0.974	253.887		±0.002	-	-	2700	-	5.3	+0.6, -0.3	22	-90	-	-	-	-	-
J1902+0248	36.738	-1.249	272		±0.1	-	-	8.06	-	5.6	+0.7, -0.3	18	-122	-	-	-	-	-
J1853+0505	37.65	1.956	279		±3	-	-	11.2	-	6.4	+1.0, -0.5	7	218	-	-	-	-	-
J1902+02	35.917	-1.436	281.2		±0.01	-	-	-	-	6	+0.8, -0.3	-	-150	-	-	-	-	-
J1858+0319	36.714	-0.094	284		±3	-	-	134	-	4.6	+0.4	31	-8	-	-	-	-	-
J1853+03	35.78	1.02	290.2		±0.01	-	-	-	-	6	+0.7, -0.4	-	107	-	-	-	-	-
J1903+0327	37.336	-1.014	297.525		±0.006	-	-	1810	-	6.1	+0.7, -0.4	7	-108	-	-	-	-	-
J1901+0124	35.381	-1.677	314.4		±1.3	354	±5.5	1.56	1.13	6.7	+1.0, -0.5	14	-196	-	-	-	-	-
J1852+0305	35.804	1.16	320		±12	264	±15.0	206	0.83	6.5	+0.8, -0.4	8	132	-	-	-	-	-
J1858+0241	36.18	-0.43	336		±15	-	-	3.06	-	5.5	+0.5	24	-41	-	-	-	-	-
J1856+0404	37.128	0.745	341.3		±0.7	-141	±20.0	180	-0.41	5.9	+0.7, -0.4	11	77	-	-	-	-	-
J1901+0413	37.806	-0.232	352		±3	213.6	±5.6	0.321	0.61	5.5	+0.5	7	-22	-	-	-	-	-
J1858+0346	37.083	0.182	386		±1	-	-	1.99	-	5.7	+0.5	17	18	-	-	-	-	-
J1901+0320	36.999	-0.613	393		±7	19.3	-	-	6.8	+0.9	8	-73	-	-	-	-	-	-
J1901+0331	37.213	-0.637	402.08		±0.012	-237.4	±1.5	1.39	-0.59	7	+1.0	3.6 ¹ , 3.6	-78	-	-	-	-	-
J1855+0307	36.167	0.533	402.5		±1.9	69.2	±4.6	0.74	0.17	6.8	+1.0, -0.8	8	63	-	-	-	-	-
J1854+0311	36.209	0.824	404		±8	-	-	11.7	-	7.1	+1.0, -0.8	22	102	-	-	-	-	-
J1901+0234	36.37	-1.048	404		±3	-	-	0.609	-	7.2	+1.2, -0.8	20	-132	-	-	-	-	-
J1851+0118	34.153	0.504	418		±7	-	-	0.105	-	7	+1.0	24	62	-	-	-	-	-
J1859+040	34.401	-1.587	420		±3	-	-	-	-	8	+2.0	3	-222	-	-	-	-	-
J1855+0422	37.314	-1.032	438		±6	-	-	28.6	-	7.8	+1.5, -1.0	11	143	-	-	-	-	-
J1854+0319	36.179	0.947	480.2		±12	-	-	181	-	8.3	+2.0, -1.0	18	142	-	-	-	-	-
J1858+02	35.46	-0.547	492.1		±0.01	-	-	-	-	7.5	+1.5, -1.0	-	-	-	-	-	-	-
J1857+0212	35.617	-0.39	506.77		±1.18	423	±21.0	0.164	0.83	7.7	+1.5, -1.0	6	-52	-	-	-	-	-
J1850+0242	35.265	1.403	540.068		±0.009	-	-	0.437	-	12	+3.0, -2.0	-	294	-	-	-	-	-
J1901+0355	37.58	-0.444	547		±3	-	-	0.69	-	8	+1.5, -1.2	19	-62	-	-	-	-	-
J1853+044	36.671	1.476	549.3		±1.3	-	-	-	-	11.5	+3.0	-	296	-	-	-	-	-
J1856+0102	34.54	-0.524	554		±3	556.9	±8.2	8.04	1.01	8.1	+2.0, -1.0	12	-92	-	-	-	-	-
J1851+0233	35.181	1.232	606		±4	-	-	2.5	-	13	+3.0, -2.5	26	280	-	-	-	-	-
J1856+0245	36.008	0.057	623.5		±0.2	-	-	0.0206	-	7	+1.0	10	7	-	-	-	-	-
J1855+0306	36.175	0.483	634		±6	-	-	3.71	-	9	+2.0	31	76	-	-	-	-	-
J1857+0300	36.274	0.072	691		±4	-	-	4.62	-	7.3	+1.0	33	9	-	-	-	-	-
J1858+0215	35.725	-0.493	702		±0.1	-	-	2.56	-	10	+2.5	16	-86	-	-	-	-	-
J1857+0210	35.586	-0.493	783		±11	-	-	0.712	-	11	+3.0	14	-75	-	-	-	-	-
J1855+0205	35.281	0.007	867.3		±0.2	-	-	60.5	-	8	+1.5, -1.0	17	1	-	-	-	-	-

Table A10. Radio pulsars in the solid angle interval $38^\circ < \ell < 42^\circ$; $-2^\circ < b < 2^\circ$ with measured DM. See Table 1 for column descriptions.

PSR	Data from ATNFPC							Adopted and Calculated Data in this Study										
	ℓ degree	b degree	DM pc/cm ³	err pc/cm ³	RM rad/m ²	err rad/m ²	τ Myr	RMDM kpc	err kpc	d_{Crab} kpc	z	RMDM kpc	err kpc	d_{Crab} kpc	z			
J1908+0734	41.585	-0.27	11.104		±0.011	-19	±18.0	4.08	-1.71	0.7	+0.2	25.1 ¹ , 10.2	-3	-	-	-	-	-
J1905+0400	38.095	-1.289	25.6923		±0.0012	-	-	12200	-	1.1	+0.2	33	-25	-	-	-	-	-
J1909+0641	40.941	-0.94	36.7		±0.2	-	-	3.65	-	1.3	+0.2	22	-21	-	-	-	-	-
J1907+0602	40.182	-0.894	82.1		±1.1	-	-	0.0195	-	2.2	+0.5, -0.4	128	-34	-	-	-	-	-
J1901+0221	39.687	-0.13	92		±7	-229	±13.0	72.8	-2.44	2.5	+0.5	11	33	-	-	-	-	-
J1906+0509	39.291	-1.083	99.5		±1.9	-	-	1.21	-	2.8	+0.5	60.5 ¹ , 18.1	-53	-	-	-	-	-
J1902+0723	40.742	0.984	105		±0.3	-272	±30.0	36.8	-2.59	3	+0.5	18	52	-	-	-	-	-
J1910+0714	41.52	-0.87	124.06		±0.05	158	±12.0	7.02	1.27	3.5	+0.5	20.2 ¹ , 12.5	-53	-	-	-	-	-
J1913+0657	41.644	-1.712	142		±3	-	-	7.04	-	5	+0.5	33	-149	-	-	-	-	-
J1906+0454	39.045	1.167	147.793		±0.002	-	-	11100	-	4	+0.5	36	-81	-	-	-	-	-
J1913+0618	41.024	-1.96	155.097		±0.003	82.00	-	82.00	-	6	+0.5	31	-205	-	-	-	-	-
J1902+0556	39.501	0.21	173.846		±0.013	-113	±11.0	0.919	-0.64	4	+0.5	12.1 ¹ , 6.8	15	-	-	-	-	-
J1904+0451	38.806	-0.787	182.705		±0.004	-	-	16900	-	4.5	+0.5	22	-62	-	-	-	-	-
J1904+0412	38.163	-0.988	185.9		±0.7	-	-	10200	-	5	+0.5, -0.8	16	-86	-	-	-	-	-
J1908+0500	39.293	-1.403	201.42		±0.02	120.6	±6.6	1.78	0.6	5	+0.5, -0.7	19 ¹ , 8.4	-122	-	-	-	-	-
J1906+0746	41.598	0.147	217.7508		±0.004	15.0	±10.0	0.113	0.69	4.5	+0.5	49.4 ¹ , 10.1	12	-	-	-	-	-
J1914+0659	41.785	-1.846	225.3		±0.2	-	-	9460	-	5	+0.5	13	-161	-	-	-	-	-
J1907+0731	41.5	-0.11	239.8		±1.3	-	-	0.313	-	4.8	+0.5	13	-18	-	-	-	-	-
J1905+0709	40.944	0.065	245.34		±0.1	272.7	±4.4	2.08	1.11	4.9	+0.5	5	6	-	-	-	-	-
J1906+0649	40.69	-0.152	249		±4	-15.9	±9.7	1.34	-0.06	5	+0.5	14	-13	-	-	-	-	-
J1901+0716	40.569	1.056	252.81		±0.07	282	±13.0	4.46	1.12	5.5	+0.5	23.7 ¹ , 7.9	101	-	-	-	-	-
J1905+0616	40.069	-0.169	256.05		±0.01	136.5	±6.1	0.116	0.53	5	+0.5	66.3 ¹ , 10.5	-15	-	-	-	-	-
J1859+0601	39.245	0.903	276		±7	-	-	0.649	-	5.8	+0.6	14	91	-	-	-	-	-
J1904+0738	41.18	0.68	278.32		±0.08	-	-	8.06	-	5.8	+0.5, -0.7	16	69	-	-	-	-	-
J1910+0728	41.74	-0.772	283.7		±0.4	550	±11.0	0.621	1.94	5.8	+0.6	8	-78	-	-	-	-	-
J1910+0511	39.838	-1.835	300		±2	-	-	6.68	-	6	+0.6	11	-192	-	-	-	-	-
J1859+07	40.022	1.514	303		±2	-	-	-	-	5.9	+0.6	-	156	-	-	-	-	-
J1907+0345	38.075	-1.796	311.7		±0.99	426.9	±4.6	0.463	1.37	6.2	+0.5, -0.7	18	-194	-	-	-	-	-
J1900+0634	39.808	0.995	323.4		±1.8	-	-	1.21	-	6.3	+0.5	15	109	-	-	-	-	-
J1905+0654	40.502	0.388	329		±7	-	-	1.18	-	6.5	+0.5, -0.7	23	44	-	-	-	-	-

Table A14. Radio pulsars in the solid angle interval $54^\circ < \ell < 58^\circ$; $-2^\circ < b < 2^\circ$ with measured DM. See Table 1 for column descriptions.

PSR	Data from ATNFPC							Adopted and Calculated Data in this Study				
	ℓ degree	b degree	DM pc/cm ³	err pc/cm ³	RM rad/m ²	err rad/m ²	τ Myr	RM/DM	d kpc	err kpc	d_{Crab} kpc	z pc
J1929+2121	56.117	1.751	66	± 12	-	-	5.36	-	2	+0.8,-0.4	16	61
J1939+2134	57.509	-0.29	71.0237	± 0.0013	7.73	± 0.1	235	0.11	2.1	+0.4,-0.6	37.2	-11
J1938+2213	57.903	0.308	91	± 3	-	-	0.062	-	2.5	± 0.5	47 [†] , 9.7	13
J1946+2052	57.657	-1.975	93.965	± 0.003	-	-	292	-	4	+1.0,-0.5	30	-138
J1934+19	54.609	-0.397	97.6	± 0.01	-	-	-	-	2.6	± 0.5	24	-18
J1935+2025	56.051	-0.053	182	± 1	-	-	0.0209	-	4.5	± 0.5	11	-4
J1936+20	55.712	-0.323	205.1	± 0.01	-	-	-	-	4.8	± 0.5	-	-27
J1932+2020	55.575	0.639	211.151	± 0.011	10	± 6.0	1.01	0.05	5	+0.6,-0.5	8.7 [†] , 6.8	56
J1932+2220	57.536	1.554	219.2	± 0.5	173	± 11.0	0.0398	0.79	5.5	+0.8,-0.5	16.8 [†] , 6.8	149
J1938+2012	56.205	-0.764	236.909	± 0.005	-	-	55600	-	5.6	+0.6,-0.5	53	-75
J1926+2016	54.851	1.802	247	± 5	-	-	1.35	-	6.2	+0.8,-0.5	21	195
J1936+21	56.814	0.164	264	± 11	-	-	-	-	6	± 0.5	-	17
J1929+1955	54.879	1.018	281	± 4	-	-	1.6	-	7	± 0.6	12	124
J1930+1852	54.096	0.265	308	± 4	-	-	0.00289	-	6.7	± 0.5	31	31
J1938+2010	56.115	-0.672	327.7	± 0.8	-	-	3.2	-	8.2	+1.5,-1.0	23	-96
J1931+1952	55.134	0.451	441	± 8	-	-	78.8	-	9	+1.5,-1.0	21	71
J1926+1928	54.158	1.407	445	± 2	-	-	14.9	-	10	+2.5,-1.0	52 [†]	246
J1928+1923	54.281	1.016	476	± 14	-	-	2.04	-	10	+2.0,-1.0	9	177
J1929+19	54.173	0.568	527	± 6	-	-	-	-	11	± 1.5	-	109

Table A15. Radio pulsars in the solid angle interval $58^\circ < \ell < 62^\circ$; $-2^\circ < b < 2^\circ$ with measured DM. See Table 1 for column descriptions.

PSR	Data from ATNFPC							Adopted and Calculated Data in this Study				
	ℓ degree	b degree	DM pc/cm ³	err pc/cm ³	RM rad/m ²	err rad/m ²	τ Myr	RM/DM	d kpc	err kpc	d_{Crab} kpc	z pc
J1954+2407	61.367	-1.872	80.5	± 0.4	-	-	2.9	-	3	+1.0,-0.5	24	-98
J1946+24	60.306	-0.376	96	± 0.1	-	-	-	-	3	± 0.5	-	-20
J1946+2244	59.301	-1.07	140	± 20	2	± 20.0	23.8	0.01	5.9	+0.6,-0.4	27 [†] , 18	-110
J1950+2414	61.998	-1.169	142.0842	± 0.0031	-	-	3630	-	5.9	+0.7,-0.5	22	-120
J1939+2449	60.174	1.361	142.88	± 0.07	76.2	± 1.1	0.56	0.53	6	+1.0,-0.4	27 [†]	143
J1943+2210	58.439	-0.73	174.089	± 0.003	-	-	9170	-	7	+0.7,-0.5	37	-89
J1944+2236	58.9	-0.663	185.45	± 0.12	-	-	7680	-	7.4	+0.7,-0.5	24	-86
J1949+2306	59.931	-1.423	196.3	± 0.5	-	-	170	-	8.2	+1.2,-0.5	24	-204
J1948+2333	60.214	-1.045	198.2	± 0.8	-	-	0.617	-	8.2	+1.0,-0.4	14	-150
J1940+2245	58.629	0.127	222.4	± 1.3	-	-	0.323	-	8.2	± 0.4	19	18
J1946+2535	61.809	0.283	248.81	± 0.04	-	-	1.45	-	8.5	+0.6	11	42
J1940+2337	59.937	0.529	252.1	± 0.3	-	-	0.113	-	8.8	± 0.6	28	81
J1941+2525	61.037	1.263	314.4	± 0.4	-	-	0.227	-	13	+2.0,-1.2	15	287
J1934+2352	58.966	1.814	355.5	± 0.2	-	-	0.0216	-	14	+3.0,-2.0	30	443

Table A16. Radio pulsars in the solid angle interval $62^\circ < \ell < 66^\circ$; $-2^\circ < b < 2^\circ$ with measured DM. See Table 1 for column descriptions.

PSR	Data from ATNFPC							Adopted and Calculated Data in this Study				
	ℓ degree	b degree	DM pc/cm ³	err pc/cm ³	RM rad/m ²	err rad/m ²	τ Myr	RM/DM	d kpc	err kpc	d_{Crab} kpc	z pc
J1954+2923	65.924	0.772	7.932	± 0.007	-18	± 3.0	3950	-2.27	0.5	± 0.2	18.3 [†] , 2.6	7
J1957+2516	62.769	-1.973	44.137	± 0.003	-	-	2290	-	2	+1.0,-0.5	53	-69
J1955+2908	65.839	0.443	104.5159	± 0.0006	22.4	± 8.8	3270	0.21	4.2	± 0.5	12.1 [†] , 7.1	32
J1957+2831	65.524	-0.25	133.99	± 0.08	43.7	± 1.8	1.57	-0.31	5.3	+0.5	7	-21
J1946+2611	62.321	0.595	165	± 3	-88.7	± 1.7	0.314	-0.54	6.3	± 0.5	38.3 [†] , 9	65
J1953+2732	64.205	0.059	195.4	± 0.9	-	-	11.9	-	6.5	+0.4,-0.8	23	7
J1955+2527	62.74	-1.571	209.971	± 0.003	-	-	8470	-	8	+2.0,-1.0	14	-219
J1948+2551	62.207	0.131	289.27	± 0.05	-	-	0.345	-	8.7	± 0.6	9	20
J1952+2630	63.254	-0.376	315.338	± 0.002	-	-	76.9	-	10	± 1.0	26	-66

Table A17. Radio pulsars in the solid angle interval $66^\circ < \ell < 70^\circ$; $-2^\circ < b < 2^\circ$ with measured DM. See Table 1 for column descriptions.

PSR	Data from ATNFPC							Adopted and Calculated Data in this Study				
	ℓ degree	b degree	DM pc/cm ³	err pc/cm ³	RM rad/m ²	err rad/m ²	τ Myr	RM/DM	d kpc	err kpc	d_{Crab} kpc	z pc
J1953+30	66.57	1.306	43.61	± 0.11	-	-	-	-	2	+1.0,-0.5	-	46
J2006+3102	68.667	0.53	107.16	± 0.01	-	-	0.104	-	4.3	+0.6,-0.4	14	40
J2000+29	66.232	-0.478	132.5	± 1.4	-	-	-	-	5	+0.7,-0.5	-	-42
J2010+3051	68.967	-1.326	133.756	± 0.002	-64	± 15.0	15700	-0.48	6.2	+1.0,-0.5	24	-143
J2002+3217	69.261	0.879	142.21	± 0.03	-90.2	± 1.3	0.105	-0.63	6.4	+0.8,-0.4	20 [†] , 6.8	98
J2013+3058	69.485	-1.886	148.7	± 0.1	-	-	28.8	-	7	+1.0,-0.5	29	-221
J1952+30	66.184	1.529	188.6	± 0.6	-	-	-	-	7.5	+1.0,-0.5	-	200
J2007+3120	69.042	-0.535	191.5	± 0.2	-	-	0.618	-	7	+0.7,-0.5	21	-65
J2002+30	67.917	-0.187	196	± 38	-	-	-	-	7	± 1.0	-	-23
J1958+30	66.856	0.417	199.3	± 0.4	-	-	-	-	7.2	± 1.0	-	52
J2004+3137	69.011	0.021	234.82	± 0.008	30	± 6.0	0.449	0.13	7.8	± 0.5	12.3 [†] , 5.6	3

Table A18. Radio pulsars in the solid angle interval $70^\circ < \ell < 74^\circ$; $-2^\circ < b < 2^\circ$ with measured DM. See Table 1 for column descriptions.

PSR	Data from ATNFPC							Adopted and Calculated Data in this Study				
	ℓ degree	b degree	DM pc/cm ³	err pc/cm ³	RM rad/m ²	err rad/m ²	τ Myr	RM/DM	d kpc	err kpc	d_{Crab} kpc	z pc
J2018+3431	73.044	-0.841	222.35	± 0.07	-	-	3.34	-	8.5	+1.2,-0.8	15	-125
J2009+3326	71.103	0.124	263.6	± 0.8	-	-	15.5	-	8.2	± 0.8	19	18
J2011+3331	71.32	-0.049	298.58	± 0.06	-	-	8.27	-	8.6	± 0.9	12	-7
J2004+3429	71.425	1.571	351	± 0.1	-	-	0.0185	-	12.5	± 2.0	23	343
J2010+3230	70.391	-0.495	371.8	± 0.5	-	-	6.32	-	12	± 2.0	22	-104

Table A19. Radio pulsars in the solid angle interval $74^\circ < \ell < 78^\circ$; $-2^\circ < b < 2^\circ$ with measured DM. See Table 1 for column descriptions.

PSR	Data from ATNFPC							Adopted and Calculated Data in this Study				
	ℓ degree	b degree	DM pc/cm ³	err pc/cm ³	RM rad/m ²	err rad/m ²	τ Myr	RM/DM	d kpc	err kpc	d_{Crab} kpc	z pc
J2029+3744	76.898	-0.727	190.66	± 0.03	-6	± 1.8	1.56	-0.03	7	± 1.0	11 [†] , 9.7	-89
J2030+3641	76.123	-1.438	246	± 0.7	514	± 1.0	0.488	2.09	9.5	+1.5,-0.8	19	238
J2021+3651	75.222	0.111	367.5	± 1	524	± 4.0	0.0172	1.43	11	± 1.0	24	21
J2022+3842	76.888	0.96	429.1	± 0.5	270	± 0.1	0.00894	0.63	13	± 2.0	-	218

Table A20. Radio pulsars in the solid angle interval $78^\circ < \ell < 90^\circ$; $-2^\circ < b < 2^\circ$ with measured DM. In the first column J–Name of the pulsar is given. The second and third columns are galactic latitude (ℓ) and longitude (b) of the pulsar in degrees. The fourth and fifth columns are dispersion measure (DM) values and their error in pc/cm³. The sixth and seventh columns are rotation measure (RM) values and their error in rad/m². The eighth column is the characteristic ages (τ) of the pulsars in Myr. The ninth column is the ratio of rotation measure to dispersion measure (RM/DM). The tenth and eleventh columns are the adopted distances (d) and their error in kpc. The twelfth column is the Crab limit for the distance (d_{Crab}) in kpc. The thirteenth column is the distance to the Galactic plane (z) calculated from the adopted distance in pc. The symbol [†] indicates the Crab (S400) luminosity limit. The symbol * indicates distance and distance error from parallax (Deller et al. (2019)).

PSR	Data from ATNFPC							Adopted and Calculated Data in this Study				
	ℓ degree	b degree	DM pc/cm ³	err pc/cm ³	RM rad/m ²	err rad/m ²	τ Myr	RM/DM	d kpc	err kpc	d_{Crab} kpc	z pc
J2053+4650	86.861	1.302	98.0828	± 0.0006	-174	± 11.0	1160	-1.77	-	-	-	39
J2032+4127	80.224	1.028	114.67	± 0.04	215	± 1.0	0.201	1.87	1.5	± 0.2	-0.1	-27
J2113+4644	89.003	-1.266	141.26	± 0.09	-218.7	± 0.1	22.5	-1.55	2.2*	+0.36,-0.32*	3.1 [†] , 1.7	-49

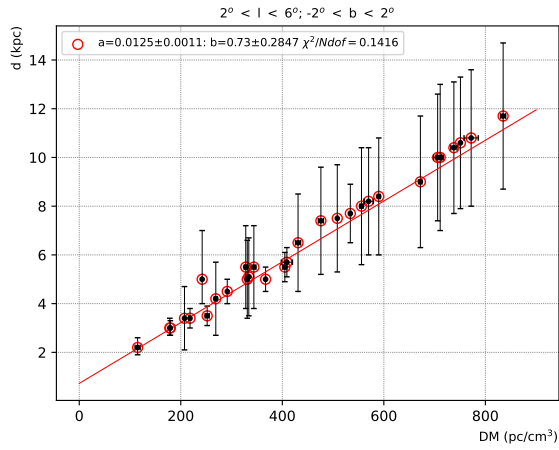


Figure A1. Distance-DM relation for radio pulsars in the solid angle interval $2^\circ < \ell < 6^\circ$; $-2^\circ < b < 2^\circ$. The data are fit to a linear function (shown in red) with a slope a , and an intercept b .

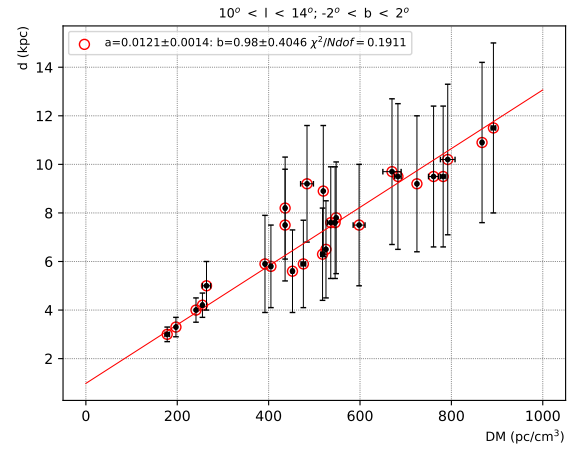


Figure A3. Distance-DM relation for radio pulsars in the solid angle interval $10^\circ < \ell < 14^\circ$; $-2^\circ < b < 2^\circ$. The data are fit to a linear function (shown in red) with a slope a , and an intercept b .

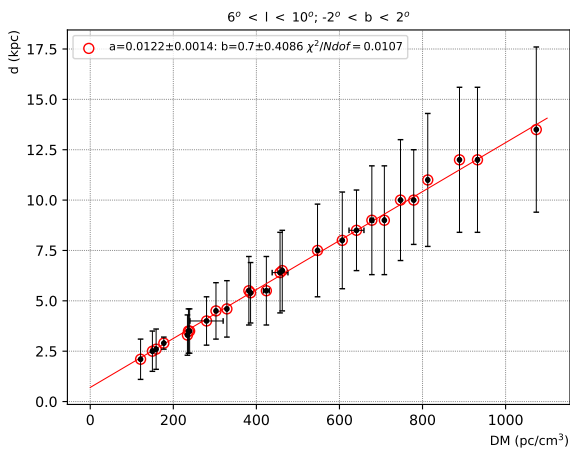


Figure A2. Distance-DM relation for radio pulsars in the solid angle interval $6^\circ < \ell < 10^\circ$; $-2^\circ < b < 2^\circ$. The data are fit to a linear function (shown in red) with a slope a , and an intercept b .

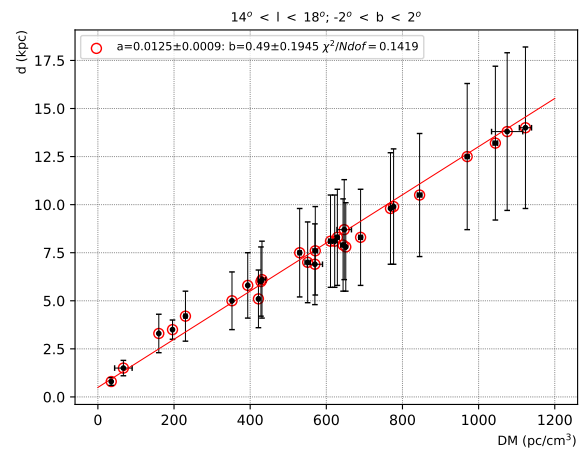


Figure A4. Distance-DM relation for radio pulsars in the solid angle interval $14^\circ < \ell < 18^\circ$; $-2^\circ < b < 2^\circ$. The data are fit to a linear function (shown in red) with a slope a , and an intercept b .

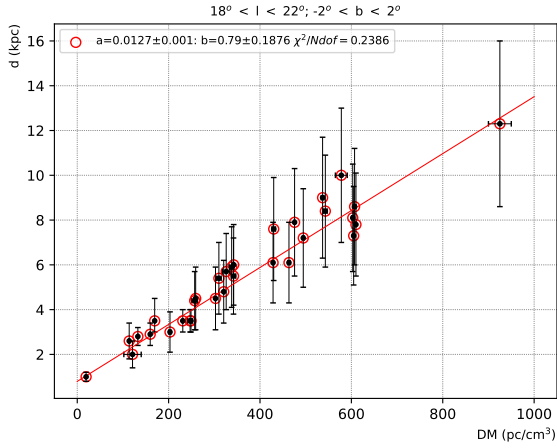


Figure A5. Distance-DM relation for radio pulsars in the solid angle interval $18^\circ < \ell < 22^\circ$; $-2^\circ < b < 2^\circ$. The data are fit to a linear function (shown in red) with a slope a , and an intercept b .

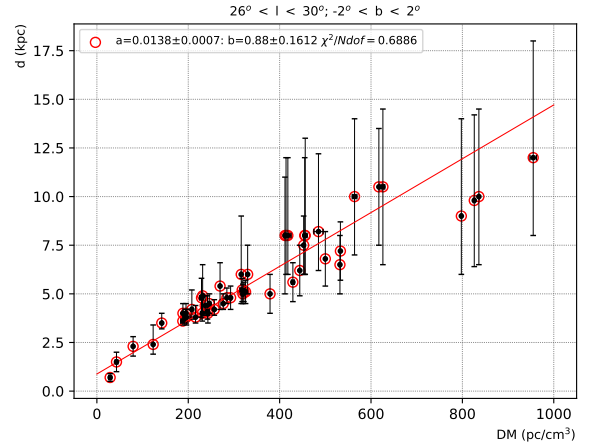


Figure A7. Distance-DM relation for radio pulsars in the solid angle interval $26^\circ < \ell < 30^\circ$; $-2^\circ < b < 2^\circ$. The data are fit to a linear function (shown in red) with a slope a , and an intercept b .

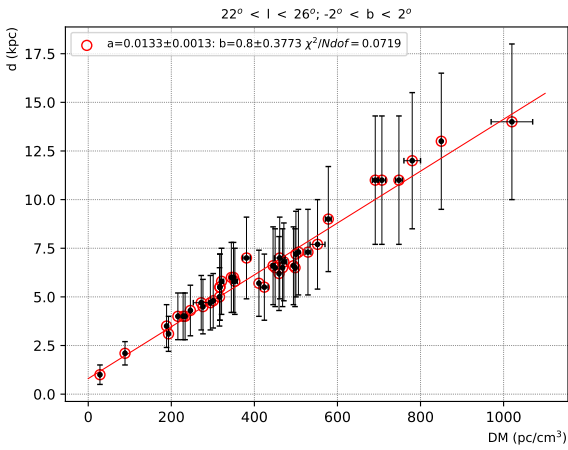


Figure A6. Distance-DM relation for radio pulsars in the solid angle interval $22^\circ < \ell < 26^\circ$; $-2^\circ < b < 2^\circ$. The data are fit to a linear function (shown in red) with a slope a , and an intercept b .

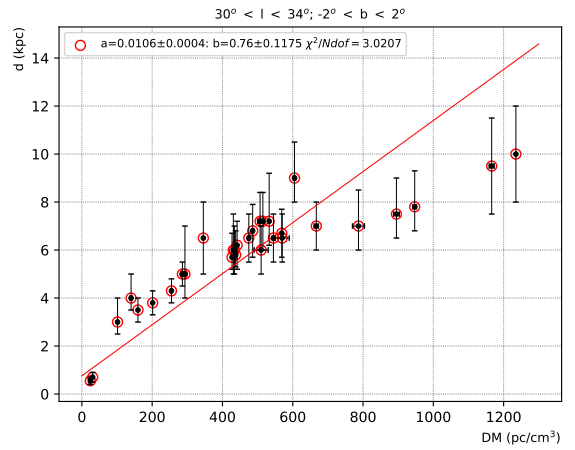


Figure A8. Distance-DM relation for radio pulsars in the solid angle interval $30^\circ < \ell < 34^\circ$; $-2^\circ < b < 2^\circ$. The data are fit to a linear function (shown in red) with a slope a , and an intercept b .

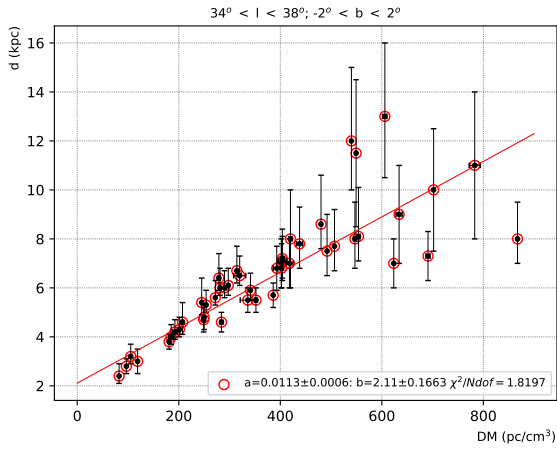


Figure A9. Distance-DM relation for radio pulsars in the solid angle interval $34^\circ < \ell < 38^\circ$; $-2^\circ < b < 2^\circ$. The data are fit to a linear function (shown in red) with a slope a , and an intercept b .

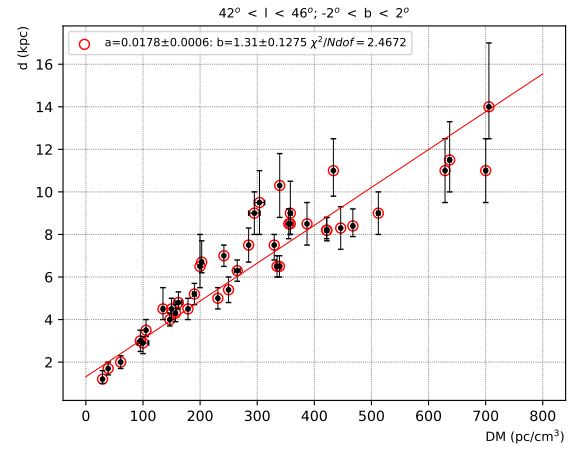


Figure A11. Distance-DM relation for radio pulsars in the solid angle interval $42^\circ < \ell < 46^\circ$; $-2^\circ < b < 2^\circ$. The data are fit to a linear function (shown in red) with a slope a , and an intercept b .

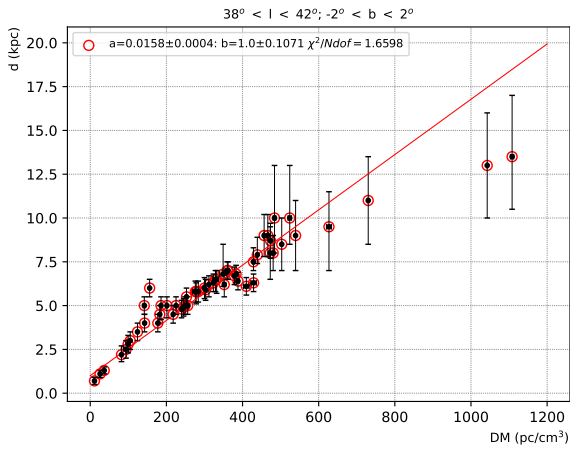


Figure A10. Distance-DM relation for radio pulsars in the solid angle interval $38^\circ < \ell < 42^\circ$; $-2^\circ < b < 2^\circ$. The data are fit to a linear function (shown in red) with a slope a , and an intercept b .

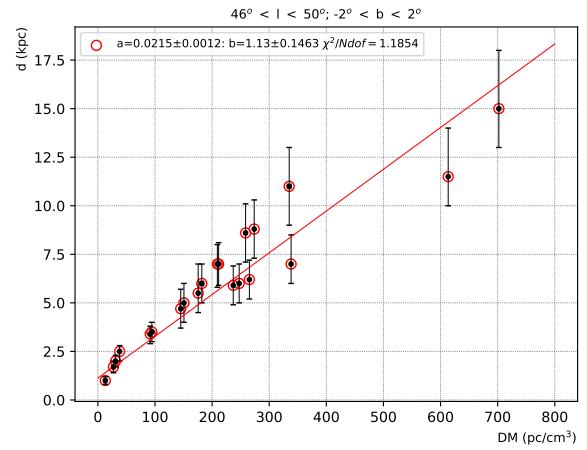


Figure A12. Distance-DM relation for radio pulsars in the solid angle interval $46^\circ < \ell < 50^\circ$; $-2^\circ < b < 2^\circ$. The data are fit to a linear function (shown in red) with a slope a , and an intercept b .

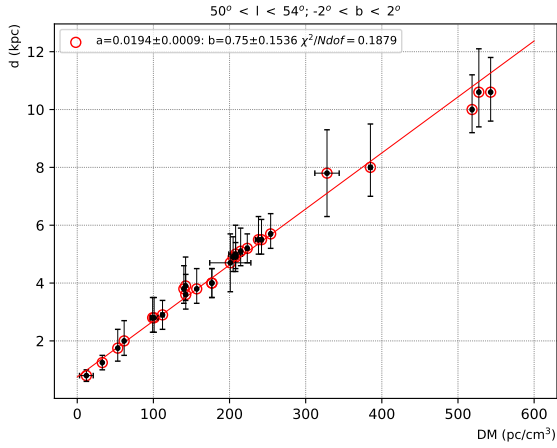


Figure A13. Distance-DM relation for radio pulsars in the solid angle interval $50^\circ < \ell < 54^\circ$; $-2^\circ < b < 2^\circ$. The data are fit to a linear function (shown in red) with a slope a , and an intercept b .

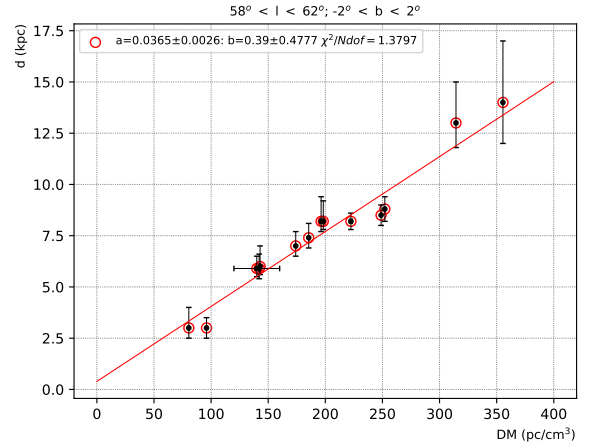


Figure A15. Distance-DM relation for radio pulsars in the solid angle interval $58^\circ < \ell < 62^\circ$; $-2^\circ < b < 2^\circ$. The data are fit to a linear function (shown in red) with a slope a , and an intercept b .

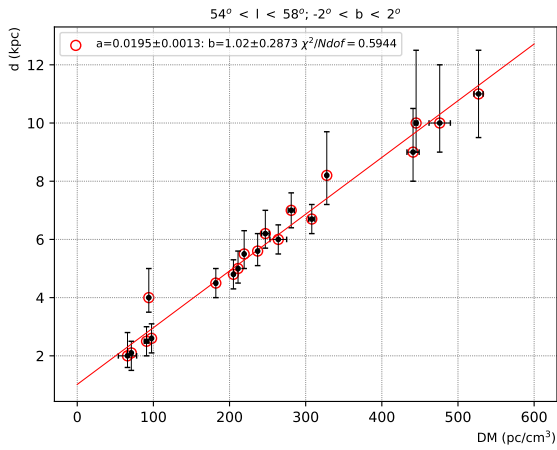


Figure A14. Distance-DM relation for radio pulsars in the solid angle interval $54^\circ < \ell < 58^\circ$; $-2^\circ < b < 2^\circ$. The data are fit to a linear function (shown in red) with a slope a , and an intercept b .

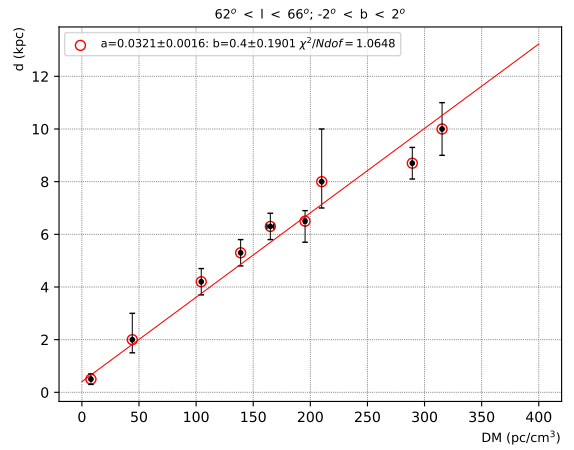


Figure A16. Distance-DM relation for radio pulsars in the solid angle interval $62^\circ < \ell < 66^\circ$; $-2^\circ < b < 2^\circ$. The data are fit to a linear function (shown in red) with a slope a , and an intercept b .

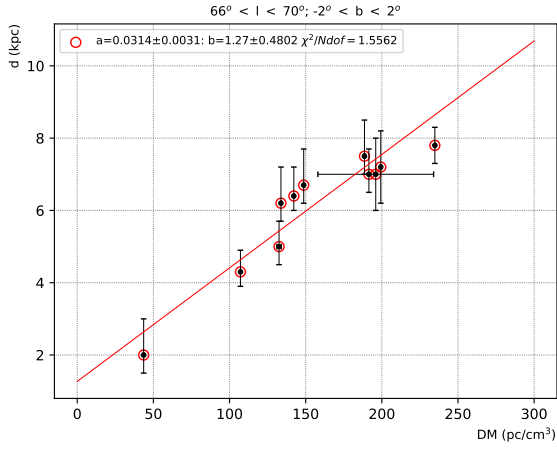


Figure A17. Distance-DM relation for radio pulsars in the solid angle interval $66^\circ < \ell < 70^\circ$; $-2^\circ < b < 2^\circ$. The data are fit to a linear function (shown in red) with a slope a , and an intercept b .

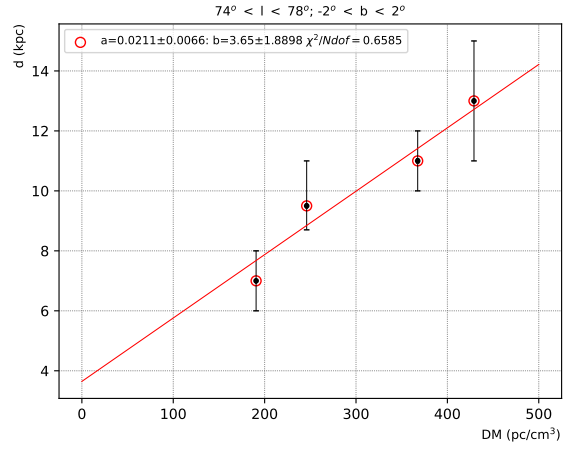


Figure A19. Distance-DM relation for radio pulsars in the solid angle interval $74^\circ < \ell < 78^\circ$; $-2^\circ < b < 2^\circ$. The data are fit to a linear function (shown in red) with a slope a , and an intercept b .

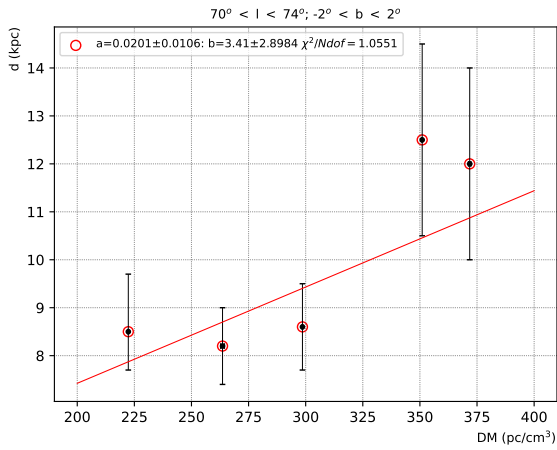


Figure A18. Distance-DM relation for radio pulsars in the solid angle interval $70^\circ < \ell < 74^\circ$; $-2^\circ < b < 2^\circ$. The data are fit to a linear function (shown in red) with a slope a , and an intercept b .